


GEOLOGI FOR SAMFUNNET

GEOLOGY FOR SOCIETY



Report no.: 2010.054		ISSN	Grading: Confidential to 30.09.2015	
Title: Quantitative assessment of geothermal resources in the Oslo and Bergen Regions				
Authors: Christophe Pascal, Marianne Aarseth, Jörg Ebbing, Torleif Lauritsen, Ole Lutro and Odleiv Olesen			Client: Statoil ASA	
County: Hordaland, Oslo			Commune:	
Map-sheet name			Number of pages: 54 Price (NOK): 200,- Map enclosures:	
Fieldwork carried out: 2009	Date of report: 30.09.2010	Project no.: 3305.00	Person responsible: 	
<p>Summary:</p> <p>The geothermal potential of Norway mainland remains unknown. One of the major outcomes of the Kontiki project (2004-2007) was that heat flow values in southern Norway were, at least, 10 mW/m² higher than previously thought, opening the perspective for a future use of geothermal energy. A very first attempt was made to estimate underground temperatures well below the deepest levels reached by the scientific drillholes. The study suggested favourable conditions mostly in the Oslo Region but the error bars associated with the temperature determinations were deemed large. In the present project we aim to explore the potential for use of geothermal energy in the most populated areas of Norway: Oslo/Asker and Bergen/Mongstad. A relatively large amount of data has already been collected in the Oslo Region in the course of various NGU projects. In contrast, the Bergen and Mongstad areas were not covered by any kind of geothermal data at the start of the present project. We conducted the very first gamma spectrometry study in the Bergen and Mongstad areas in order to assess the heat productivity of the basement. For the Oslo Region we used and completed the existing data in order to model the 3D thermal state at depth.</p> <p>Most rocks in the Bergen and Mongstad areas show typical of the Norwegian basement (i.e. 1 to 3 μW/m³) to low (i.e. less than 1 μW/m³) heat generation values. The rocks in the vicinity of the Mongstad refinery have almost no heat generation at all, suggesting that medium to high enthalpy geothermal systems are not of economic use there. The finding of very high heat generation rates (i.e. ~9 μW/m³) for the Løvestakken Granite, five kilometres southwest of Bergen downtown, is the most unexpected result of the study. The data suggests that the Løvestakken Granite is the most radioactive granite ever measured in Norway. Conservative estimates lead to temperature gradients between 27 °C/km and 43°C/km and temperatures between 135°C and 215°C at 5 km depth, implying that economic temperatures may prevail below all of the municipality of Bergen. Our "Preferred" modelling scenario for the Oslo Region suggests temperatures between 30°C and 34°C at ~1 km depth. Temperatures in the range between 105°C and 110°C are predicted at ~5 km depth. The most robust modelling result is the relative lateral homogeneity in temperatures at 5 km depth, making site selection a less important factor when attempting to mine those depths. More significant lateral variations in temperature (i.e. 28% to 37%) are, however, predicted at 1 km depth for the whole modelled domain, indicating that selection of the drilling site is a more critical factor for exploiting the shallow geothermal resource.</p> <p>A major conclusion of this study is that deep (i.e. ~5 km) temperatures, in the Oslo Region, remain relatively modest in all modelled cases and merely not of economic use with the present-day technology at hand. Temperatures at shallow depths appear high enough to be used for e.g. heating purposes.</p>				
Keywords: Geofysikk (Geophysics)		Geotermi (Geothermy)	Modellering (Modelling)	
Magnetometri (Magnetometry)		Gravimetri (Gravimetry)	Petrofysikk (Petrophysics)	
Radiometri (Radiometry)		Fagrapport (Scientific report)		

CONTENTS

1	INTRODUCTION	7
2	SYNOPSIS.....	9
2.1	Objectives of the study	9
2.2	Heat generation from basement rocks of the Bergen/Mongstad areas	9
2.3	3D thermal modelling of the Oslo Region	12
3	RADIOMETRIC MEASUREMENTS IN THE BERGEN AND MONGSTAD AREAS	15
3.1	Method.....	15
3.2	Heat generation in the Bergen and Mongstad areas	16
3.3	Summary and outlook	18
4	RADIOMETRIC AND BOREHOLE DATA IN THE OSLO REGION	21
4.1	Airborne radiometrics and natural heat generation	21
4.2	Information gained from the Rikshospitalet, Arnestad and Hamar boreholes	24
4.2.1	Rikshospitalet borehole	24
4.2.2	Arnestad borehole	24
4.2.3	Hamar borehole	25
4.3	Conclusions	26
5	3D CRUSTAL MODELLING (OSLO-ASKER)	27
5.1	Data	27
5.1.1	Petrophysics	27
5.1.2	Gravity data	28
5.1.3	Magnetic data	29
5.1.4	Seismic data.....	30
5.2	Potential field anomalies and surface geology	31
5.3	3D modelling	32
5.4	Conclusions	36
6	3D THERMAL MODELLING (OLSO-ASKER)	39
6.1	Introduction	39
6.2	Modelling strategy	39
6.3	Modelling results	41
6.4	Conclusions	46
7	CONCLUSIONS AND RECOMMENDATIONS	49
8	REFERENCES	51
9	APPENDIX A: LITHOLOGIES PENETRATED IN THE RIKSHOSPITALET BH3 DRILLHOLE	53

1 INTRODUCTION

The geothermal potential of Norway mainland remains unknown. The very first heat flow studies conducted in the 70s concluded that heat flow in Norway was extremely low and characterised by values of 40 to 50 mW/m^2 , typical for cratonic areas (Haenel et al. 1979). Although previous data were collected at shallow depths in mining drillholes or at the bottom of lakes and were not corrected for paleoclimatic disturbances, this statement has been taken as valid during the past decades (i.e. Hurter and Haenel 2002). The Kontiki project (2004-2007, Olesen et al. 2007), supported by Statoil, was designed with the aim of improving our knowledge on the thermal state of the Norwegian crust onshore and with the final goal of extrapolating this knowledge to the sedimentary basins offshore. One of the major achievements of the study was the demonstration that heat flow values in southern Norway were, at least, 10 mW/m^2 higher than previously thought (Fig. 1.1).

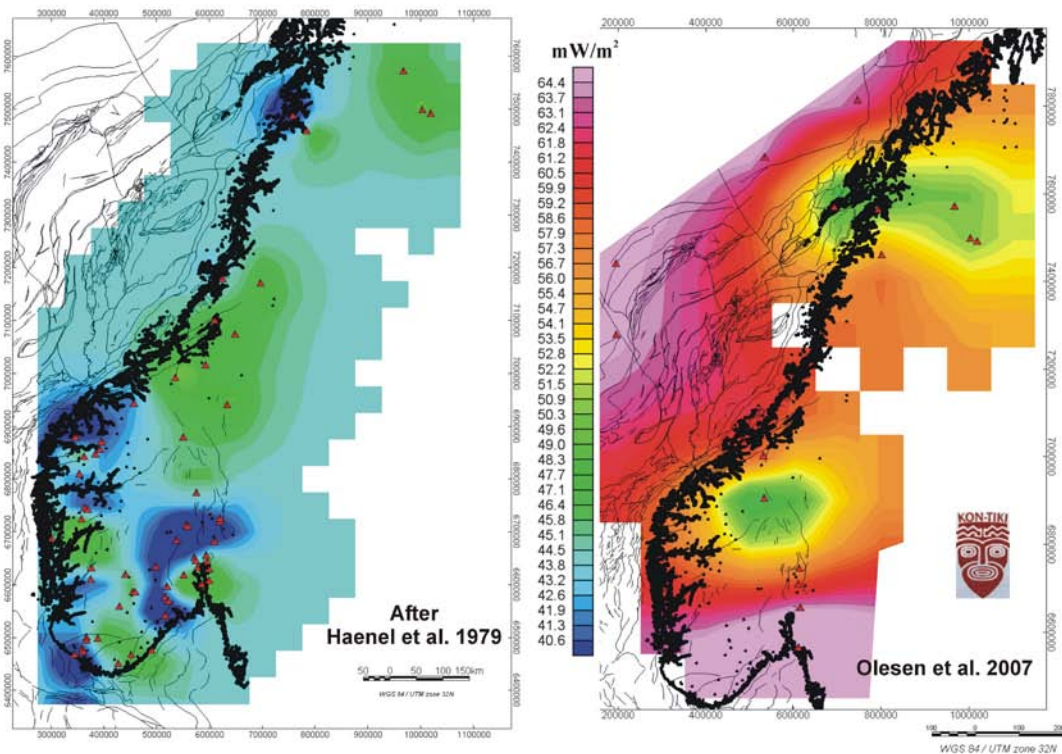


Figure 1.1. Heat flow maps after Haenel et al. (1979) and Olesen et al. (2007). Note the dramatic change in heat flow values between old and uncorrected data and modern heat flow data.

An obvious implication of the revised heat flow map is that underground temperatures are much higher than previously anticipated (Pascal et al. 2010, Fig. 1.2), opening perspectives for a future use of geothermal energy in Norway. A major progress in our understanding of the thermal state of the Norwegian crust has been made during the Kontiki project (Olesen et al. 2007). However, in order to assess the economic potential of geothermal resources in Norway more focused studies are needed. Pascal et al. (2010) made the very first attempt to

estimate underground temperatures well below the deepest levels reached by the scientific drillholes. Their analysis points to favourable conditions mostly in the Oslo Region but error bars remain large (Fig. 1.2).

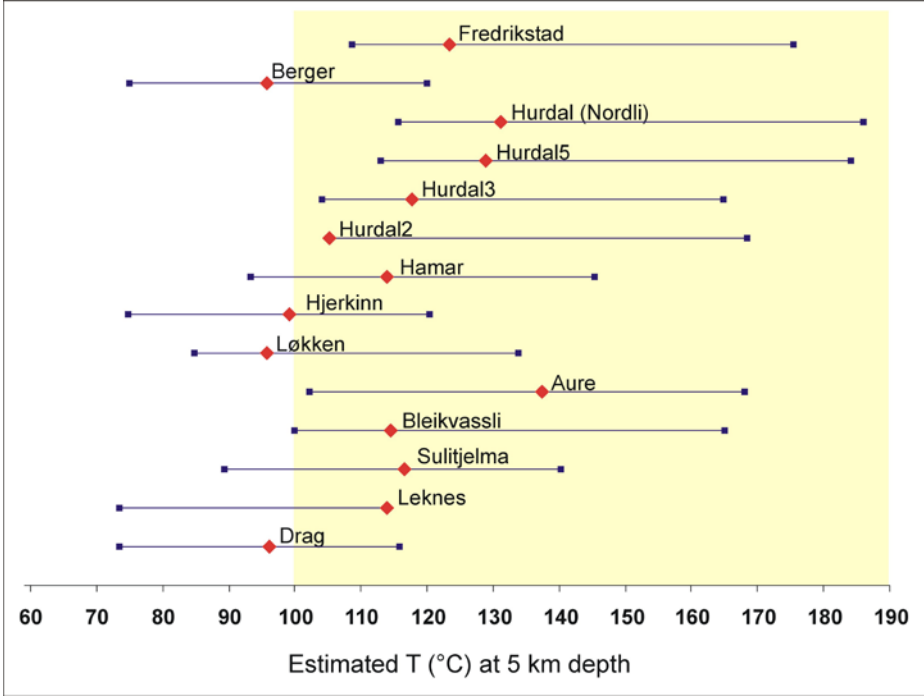


Figure 1.2. Estimated temperatures at 5 km depth for the Kontiki heat flow sites. Note that despite large error bars the analysis predicts more favourable conditions in the Oslo Region (after Pascal et al. 2010).

In the present project we propose to refine these previous estimates and to target the most populated areas of Norway: Oslo and Bergen, including the area of Mongstad. A relatively large amount of data has already been collected in the former region whereas a crucial lack of geothermal data characterises the later one. We aim (1) to conduct a “first ever” gamma spectrometry study in the Bergen/Mongstad Region in order to assess the heat productivity of the basement and (2) to use and complete the data at hand and to model the 3D thermal configuration of the underground of the Oslo Region. We summarise the major outcomes and implications of the project in Chapter 2. The following chapters give a detailed and more technical description of the methods and approaches used.

2 SYNOPSIS

2.1 Objectives of the study

We aim to explore the potential for use of geothermal energy in the most populated areas of Norway: Oslo and Bergen/Mongstad. A relatively large amount of data has already been collected in the Oslo Region in the course of various NGU projects, including the Kontiki heat flow project financed by Statoil (Olesen et al. 2007). In contrast, the Bergen and Mongstad areas were not covered by any kind of geothermal data at the start of the present project. It was, therefore, crucial to get a preliminary assessment of the Bergen Region during the one-year duration of the project.

We conducted the “first ever” gamma spectrometry study in the Bergen and Mongstad areas in order to assess the heat productivity of the basement. For the Oslo Region we used and completed the existing data in order to model the 3D thermal configuration at depth.

2.2 Heat generation from basement rocks of the Bergen/Mongstad areas

The main goal of the ground-based gamma spectrometry measurements was to get a preliminary assessment on the geothermal potential of the Bergen and Mongstad areas. We used a handheld spectrometer in order to calculate the relative concentrations in heat-producing radioactive elements (i.e. uranium, thorium and potassium) and derive heat generation rates from the different rock units exposed at the surface (see details in Chapter 3). We made 128 measurements at 44 sites located between the Bjørnafjord in the south and the Fensfjord in the north. Most sites present normal to low concentrations in uranium and thorium, the most heat productive elements. In the neighbourhood of the Mongstad refinery, concentrations in radioactive elements were found low, resulting in negligible heat generation rates (Fig. 2.1). The low heat generation in the northern part of the studied domain is in agreement with the observed rocks involved in the present case in the Caledonian nappes. Those are mainly amphibolitic gneisses and anorthosites that are, usually, strongly depleted in radioactive elements.

High to extremely high concentrations in uranium and thorium together with high potassium content are measured southwest of Bergen, resulting in anomalously high heat generation (Fig. 2.1). The Precambrian Løvestakken Granite crops out in this specific area of the Bergen Municipality. The levels of radioactivity and hence of heat generation are surprisingly high for a 1 Ga old granite, strongly deformed during the Caledonian Orogeny (Ragnhildstveit and Helliksen 1997). Noteworthy, uranium concentrations were found high enough to result in radon hazard for the local population.

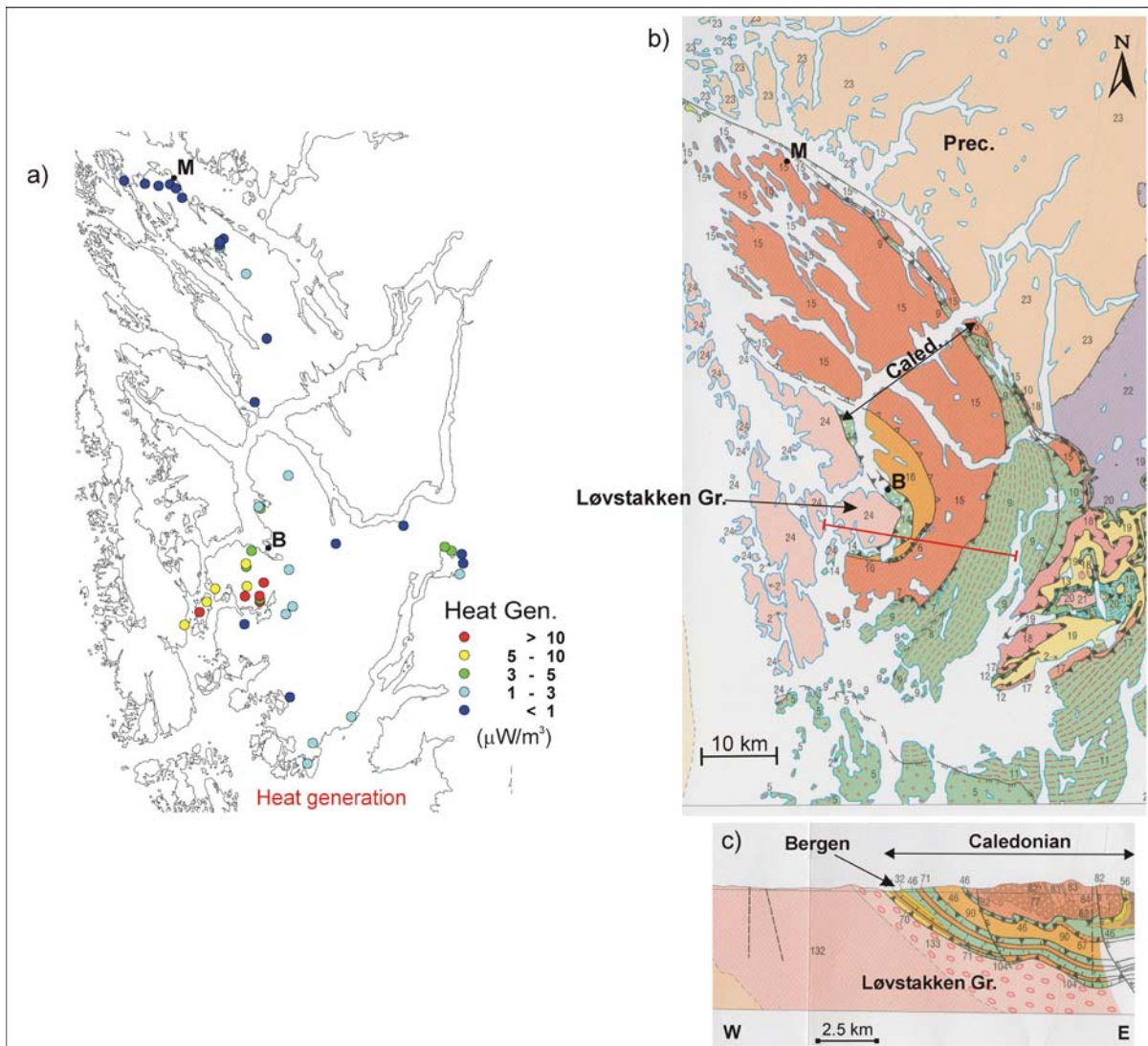


Figure 2.1. a) Heat generation values obtained from gamma spectrometry measurements. b) Simplified geological map of the Bergen Region (after Ragnhildsveit & Helliksen 1997). Pink colours in the western part depict Precambrian intrusions, including the highly radioactive Løvstakken Granite. The location of the Caledonian nappes (mainly gneisses, anorthosites and schists) is indicated. The Precambrian basement crops out in the NE and is labelled with the numbers 22 and 23. B. = Bergen, M. = Mongstad, Prec. = Precambrian and Caled. = Caledonian nappes. c) Interpretative cross section (red line in a)) suggesting that the Løvstakken Granite (rock units 132 and 133) extends eastwards and below the city of Bergen.

This preliminary study confirms that most rocks in the Bergen and Mongstad area show typical for the Norwegian basement (i.e. 1 to 3 $\mu\text{W}/\text{m}^3$) to low (i.e. less than 1 $\mu\text{W}/\text{m}^3$) heat generation values. The rocks in the vicinity of the Mongstad have almost no heat generation at all. This suggests that medium to high enthalpy geothermal systems are much too deep below the ground surface to be of economic use there.

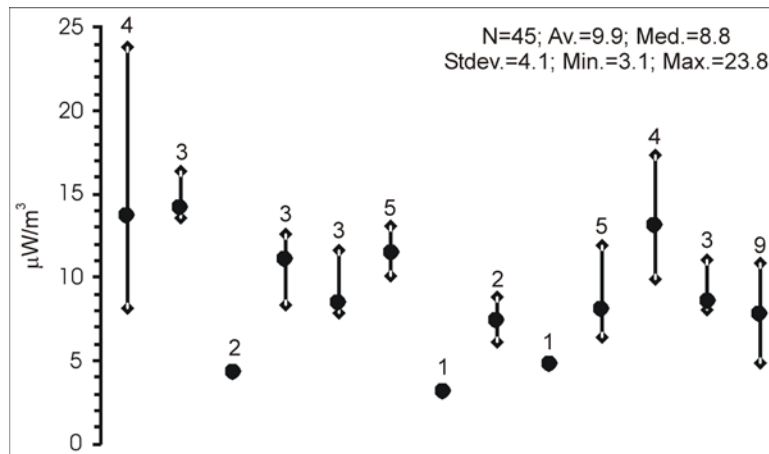


Figure 2.2. Heat generation values in $\mu\text{W}/\text{m}^3$ at the thirteen measurement sites on the Løvstakken Granite (see Fig. 2.1). The values are calculated from median concentrations in U, Th and K at each site and minima and maxima are showed. The number of measurements per site is also given. N = total number of measurements, $Av.$ = average, $Med.$ = median, $Stdev.$ = standard deviation, $Min.$ = minimum and $Max.$ = maximum.

The finding of very high heat generation rates for the Løvstakken Granite, five kilometres southwest of Bergen downtown (Fig. 2.1), represents the most unexpected result of the study. A statistical analysis of the 45 measurements taken at sites distant of up to ~ 10 km shows average and median values of 10 and 9 $\mu\text{W}/\text{m}^3$ respectively (Fig. 2.2). The data at hand suggest that the Løvstakken Granite is the most radioactive granite ever measured in Norway. It is unknown how concentrations in radioactive elements decay with depth in the Løvstakken Granite, which is primordial while attempting to estimate heat flow values and temperatures in the deep underground. Two points are, however, interesting to note. Firstly, according to the geological interpretation (Ragnhildstveit and Helliksen 1997), the granite extends to great depths and farther to the east below the Caledonian nappes. Secondly, conservative estimates using reasonable values lead to temperature gradients between 27 $^{\circ}\text{C}/\text{km}$ and 43 $^{\circ}\text{C}/\text{km}$ and temperatures between 135 $^{\circ}\text{C}$ and 215 $^{\circ}\text{C}$ at 5 km depth. The spread in values is obviously large but suggests anyway more favourable conditions for geothermal exploration with respect to most regions of Norway (Pascal et al. 2010). This implies that economic underground temperatures may prevail below all of the municipality of Bergen.

Finally it is important to note that a similar radiometric study carried out in the framework of the “North Sea Crustal Onshore-Offshore Project” (Coop, financed by a consortium of companies including Statoil) in July 2010 has confirmed and extended the results of the present study. As a follow up of the present study and as part of the Coop project, we plan (1) to use the newly acquired potential field data and to build a 2D thermal model crossing the Løvstakken Granite and (2) to drill a 1-km deep hole in order to measure temperature gradients and refine our first-order estimates.

2.3 3D thermal modelling of the Oslo Region

The goal of the 3D thermal modelling study was to determine underground temperatures in the Oslo-Asker area. In order to constrain the model, we used airborne radiometric data, temperature and lithological information from two drillholes and thermal conductivity data (see details in Chapter 4). The 3D structure of the underground was built on the basis of the geophysical modelling presented in Chapter 5 (see also Fig. 2.3). The main outcomes of the geophysical modelling are:

- the Nordmarka Igneous Complex extends farther to the south below Oslo and the Inner Oslofjord;
- the Drammen Granite has a sharp and steep eastern boundary;
- the Cambro-Silurian sediments appear to rest on the Precambrian basement;
- the Nordmarka Igneous Complex appears to be thick (more than 10 km in its middle part).

Section North

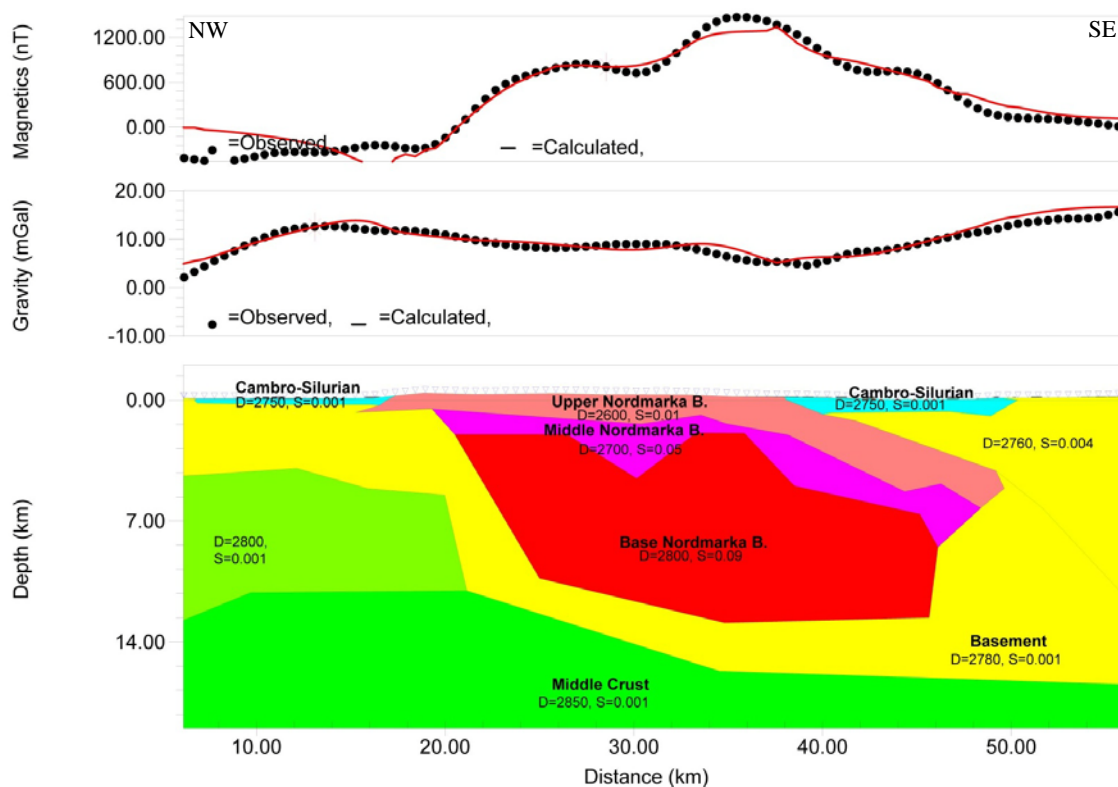


Figure 2.3. Section North of the 3D crustal model crossing the middle part of the Nordmarka Igneous Complex (see location and details in Chapter 5). Note the smooth magnetic gradient at the SE boundary of the granite indicating its extension to the east. A thin layer of Precambrian basement between the Cambro-Silurian sediments and the Nordmarka Igneous Complex has been modelled in order to account for the observed lithologies in the Rikshospitalet borehole.

The 3D thermal modelling (see Chapter 6) suggests that the highest temperatures at shallow depths (i.e. ~1 km depth) and at deeper levels (i.e. ~5 km depth) are found below the Cambro-Silurian sedimentary cover and below the locations where the upper levels of the Nordmarka Igneous Complex are the thickest, respectively. Admittedly, the resolution of the 3D geophysical crustal model degrades with depth, rendering the location of the warmest areas more uncertain at 5 km depth with respect to 1 km depth.

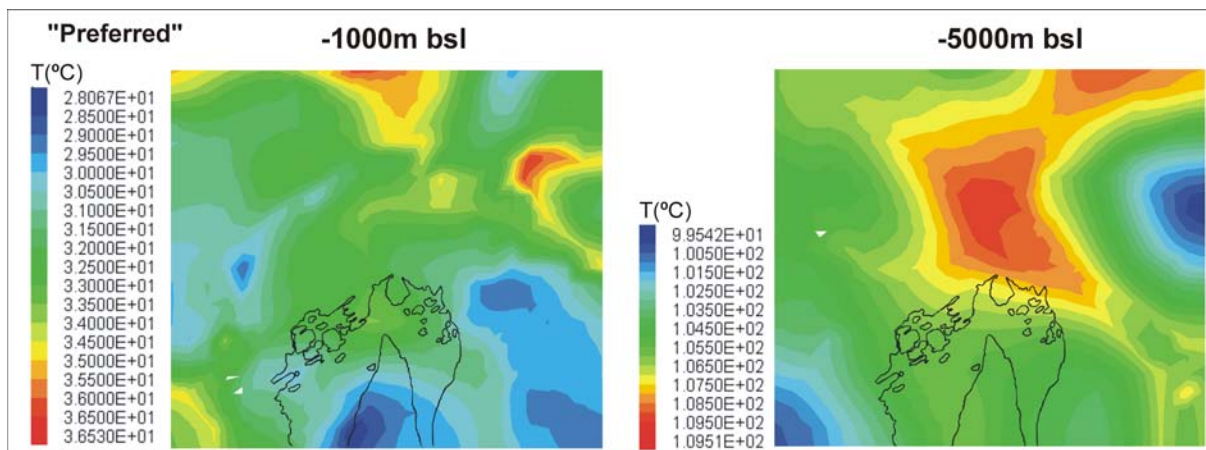


Figure 2.4. Modelled temperature distributions for the “Preferred” scenario (see Table 6.2) at 1 and 5 kilometres depth below sea-level. The apparent positive anomaly seen below the northern edge of the model at 1km bsl is partly caused by the altitude of the Nordmarka Plateau (i.e. depth below ground surface is actually 1300-1400 m there).

In detail, the thermal modelling gives some hints on the temperatures that can be encountered at depth. Our “Preferred” modelling scenario suggests temperatures between 30°C and 34°C at ~1 km depth below Oslo, Bærum and Asker, in agreement with temperature gradients measured in the Arnestad borehole and to some extent with temperatures reported for the Rikshospitalet bh3 borehole. Temperatures in the range between 105°C to 110°C are predicted at ~5 km depth. Because it is a common feature in the three modelled cases, the most robust result is the relative lateral homogeneity in temperatures at 5 km depth, making site selection a less important factor when attempting to mine those depths. More significant lateral variations in temperature (i.e. 28% to 37%) are, however, predicted at 1 km depth for the whole modelled domain, indicating that selection of the drilling site is a more critical factor for exploiting the shallow geothermal resource.

A major conclusion of this study is that deep (i.e. ~5 km) temperatures, in the Oslo Region, remain relatively modest in all modelled cases and merely not of economic use with the present-day technology at hand. Temperatures at shallow depths appear high enough to be used for e.g. heating purposes.

3 RADIOMETRIC MEASUREMENTS IN THE BERGEN AND MONGSTAD AREAS

Christophe Pascal

3.1 Method

The main goal of the radiometric measurements was to get a preliminary assessment on the geothermal potential of the Bergen and Mongstad areas, where no geothermal data were available before. We used a handheld spectrometer in order to calculate the relative concentrations in heat-producing radioactive elements (i.e. uranium, thorium and potassium) and derive heat generation rates from the different rock units exposed at the surface.



Figure 3.1. Handheld spectrometer in field (source Geological Survey of Canada).

We used the Exploranium GR-256 (Exploranium G.S. Limited), a portable 256 channel spectrometer used to record and analyse the gamma ray spectrum. The 256 channels are spread equally over the entire gamma ray spectrum of interest, thus all discrete phenomena may be studied. The GR-256 has been designed as a versatile tool for a wide range of applications including ground radiometric surveys for uranium, portable vehicle surveys for hydrocarbon, small airborne survey systems, laboratory data analysis and core logging services. The instrument is normally supplied with a 21 cubic inch detector (Fig. 3.1). The GR-256 makes gain control essentially automatic, a very critical feature for high accuracy gamma ray data analysis. It was the first spectrometer to internally store data conversion/correction constants to allow display of data in conventional counts/time period or directly in ppm eU, eTh and % K. Previous instruments were limited to typically 4 windows, often permanently located in the spectrum, to record the natural isotopes of uranium, thorium and potassium. The GR-256 allows selection of 8 windows which may be located anywhere in the spectrum with any channel width. The spectrometer manual provides more detailed information (Anonymous 1989).

The spectrometer was calibrated using NGU's calibration pads in spring 2009. The calibration method is described in Heincke et al. (2009). Measurements were taken on preferentially fresh

and regular rock faces in October 2009. We set up the measurement time to 120 seconds. Concentrations of radioactive elements were calculated using the calibration parameters and not the correction factors built in the spectrometer, the latter resulting in systematic underestimations by 2-3 ppm for U and Th and 5% for K. Heat generation rates (A in $\mu\text{W}/\text{m}^3$) are finally calculated using Rybach's formula (Rybach 1988):

$$A = \rho \cdot (9.52C_U + 2.56C_{Th} + 3.48C_K) \cdot 10^{-5} \quad (1)$$

where ρ is rock density, C_U and C_{Th} represent U and Th concentrations in ppm, respectively, and C_K represents K concentration in wt.%. In the present study, rock density is assumed to be equal to $2700 \text{ kg}/\text{m}^3$.

3.2 Heat generation in the Bergen and Mongstad areas

We made 128 measurements at 44 sites located between the Bjørnafjord in the south and the Fensfjord in the north. Most sites present normal to low concentrations in uranium and thorium (Fig. 3.2), the most heat productive elements. In particular, in the neighbourhood of the Mongstad refinery concentrations in radioactive elements are merely low, resulting in negligible heat generation rates. The low heat generation in the northern part of the studied domain is in agreement with the observed rocks involved in the present case in the Caledonian nappes (Fig. 3.3). Those are mainly amphibolitic gneisses and anorthosites that are, usually, strongly depleted in radioactive elements.

Table 3.1. U and Th concentrations determined by means of XRF analysis of one sample of the Løvstakken Granite.

Sample ID	Coordinates (UTM 32V, WGS84)	U (ppm)	Th (ppm)
Løv_1	0293954E 6694602N	$16.2 \pm 10\%$	$55.9 \pm 5\%$

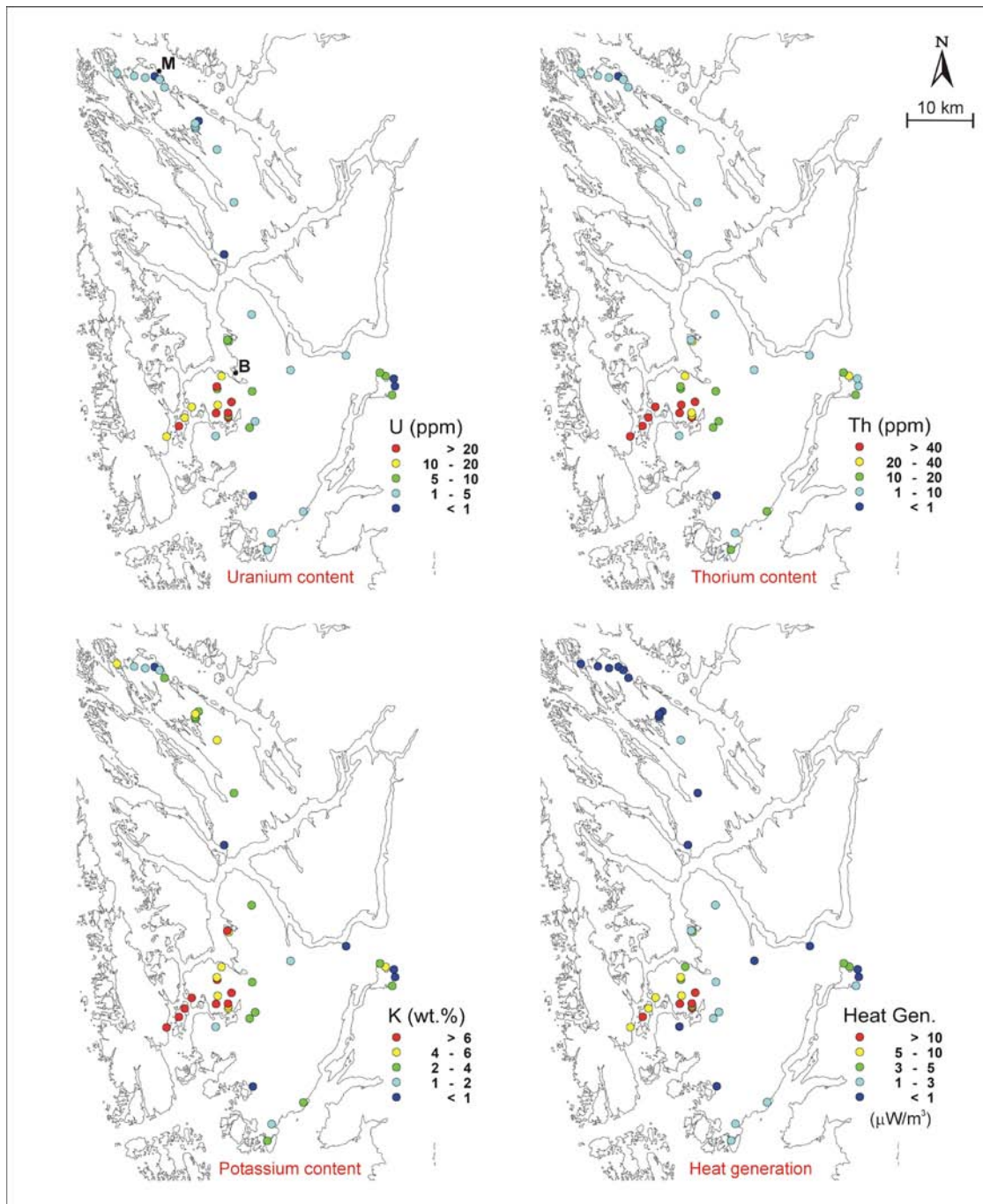


Figure 3.2. Results of the radiometric measurements: uranium, thorium and potassium concentrations and computed heat generation (dark blue = very low to low, light blue = normal levels, green = moderate to high, yellow = high to very high, red = extremely high). B=Bergen, M=Mongstad

In turn, high to extremely high concentrations in uranium and thorium together with high potassium content dominate southwest of Bergen, resulting in anomalously high heat generation (Fig. 3.2). The Precambrian Løvstakken Granite crops out in this specific area of the Bergen Region (Fig. 3.3), i.e. Bjorøy, Kråkenes, Fyllingsdalen. The levels of radioactivity and hence of heat generation are surprisingly high for a 1 Ga old granite, strongly deformed during the Caledonian Orogeny (Ragnhildstveit and Helliksen 1997). Noteworthy, uranium concentrations were found high enough to result in radon hazard for the local population. For

the sake of comparison, we sent to NGU lab one sample for XRF spectrometry analysis. The sample was collected along a very fresh road cut made during the extension of Bergen ring road in 2009. A summary of the results is given in Table 3.1., uranium and thorium concentrations appeared to be very similar to the ones derived from in-situ gamma spectrometry (Fig. 3.2).

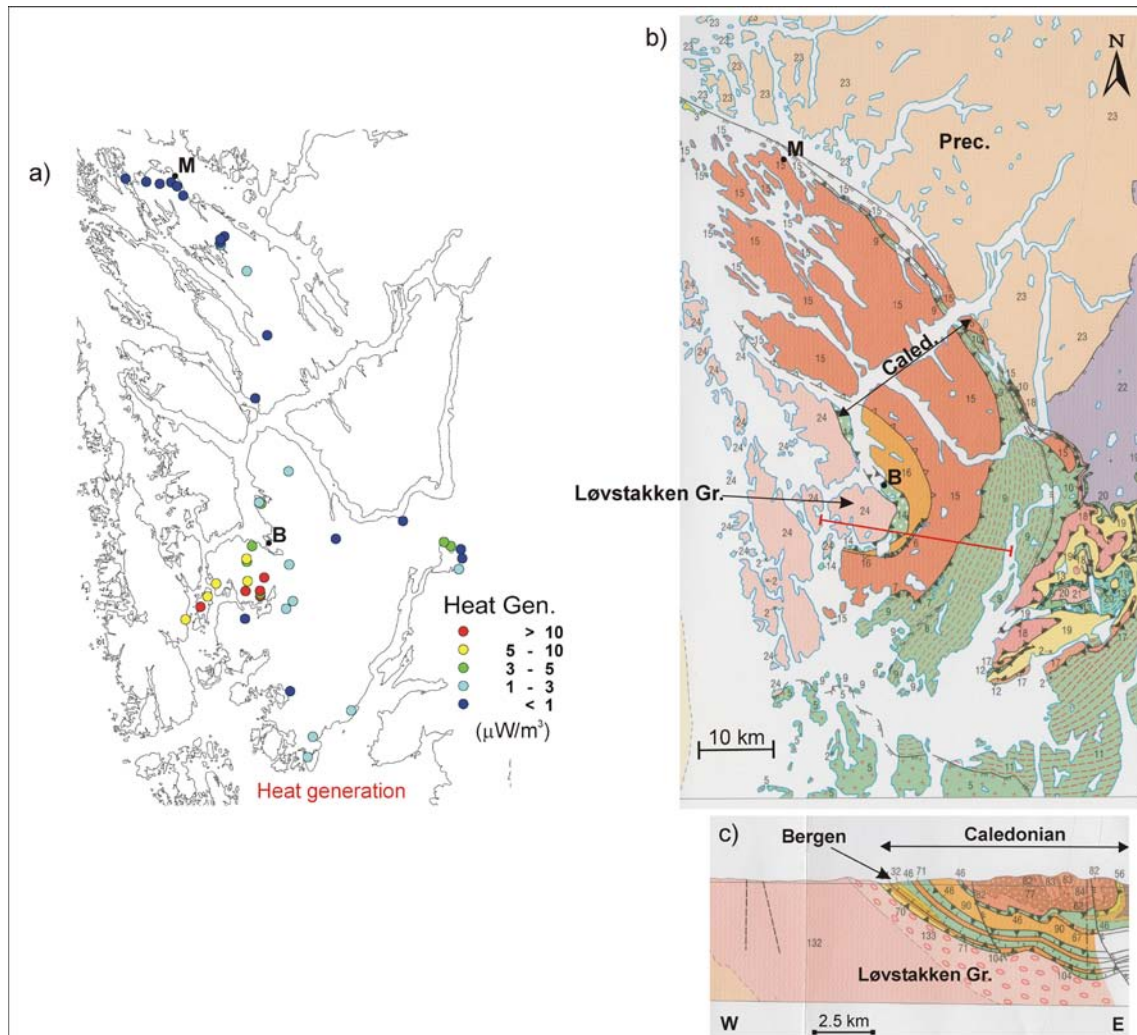


Figure 3.3. a) Heat generation values obtained from gamma spectrometry measurements. b) Simplified geological map of the Bergen Region (after Ragnhildsveit and Helliksen 1997). Pink colours in the western part depict Precambrian intrusions, including the highly radioactive Løvstakken Granite. The location of the Caledonian nappes (mainly gneisses, anorthosites and schists) is indicated. The Precambrian basement crops out in the NE and is labelled with the numbers 22 and 23. B = Bergen, M = Mongstad, Prec. = Precambrian and Caled. = Caledonian nappes. c) Interpretative cross section (red line in a)) suggesting that the Løvstakken Granite (rock units 132 and 133) extends eastwards and below the city of Bergen.

3.3 Summary and outlook

This preliminary study confirms that most rocks in the Bergen and Mongstad areas show typical of the Norwegian basement (i.e. 1 to 3 $\mu\text{W}/\text{m}^3$) to low (i.e. less than 1 $\mu\text{W}/\text{m}^3$) heat

generation values (Fig. 3.3). The rocks in the vicinity of the Mongstad refinery are mainly amphibolitic gneisses and anorthosites with almost no heat generation at all. This suggests that medium to high enthalpy geothermal systems are much too deep below the ground surface to be of economic use there. Noteworthy, the Precambrian gneissic basement underlying those rocks at depth (1-2 km?) is merely more radioactive but it is doubtful that it contributes to a significant rise in temperatures at economic depths.

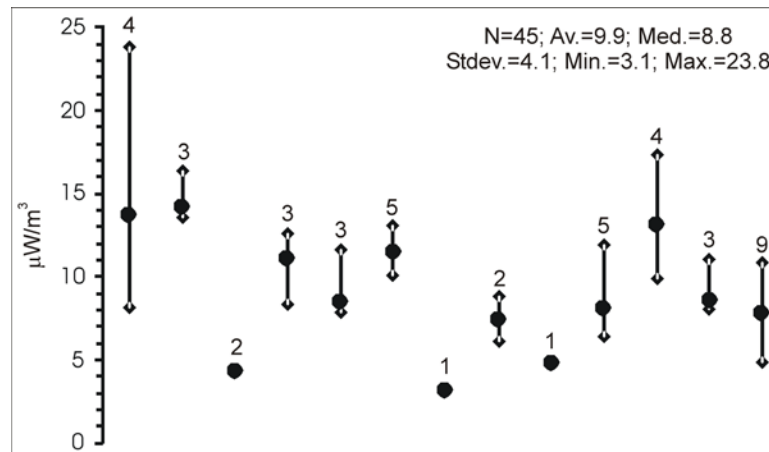


Figure 3.4. Heat generation values in $\mu\text{W}/\text{m}^3$ at the thirteen measurement sites on the Løgstakken Granite (see Fig. 3.3). The values are calculated from median concentrations in U, Th and K at each site and minima and maxima are showed. The number of measurements per site is also given. N = total number of measurements, Av. = average, Med. = median, Stdev. = standard deviation, Min. = minimum and Max. = maximum.

The finding of very high concentrations of radioactive elements and, consequently, high heat generation rates for the Løgstakken Granite, five kilometres southwest of Bergen downtown (Fig. 3.2), represents the most unexpected result of the study. A statistical analysis of the 45 measurements taken at sites distant of up to ~10 km shows average and median values of 10 and 9 $\mu\text{W}/\text{m}^3$, respectively (Fig. 3.4). In detail, a significant spread in heat generation is observed at four sites but it is attributed to variations in rock composition and, furthermore, to variable freshness of the rock faces, uranium being very sensitive to leaching by meteoritic waters. The data at hand suggests that the Løgstakken Granite is the most radioactive granite ever measured in Norway. By comparison, based on geochemical analyses and in reasonable agreement with our own radiometric determinations (see Fig. 4.1 in Chapter 4), Slagstad (2008) reports average heat generation values of 6-7 $\mu\text{W}/\text{m}^3$ for the Iddefjord Granite, one of the most radioactive plutons of the Oslo Region.

It is unknown how concentrations in radioactive elements decay with depth in the Løgstakken Granite, which is primordial while attempting to estimate heat flow values and temperatures in the deep underground. Two points are, however, interesting to note. Firstly, according to the geological interpretation (Ragnhildstveit and Helliksen 1997), the granite extends at great depths and farther to the east below the Caledonian nappes where it crops out again in a small

window at Kikedalen, ~30 km ESE of Bergen downtown. Secondly, conservative estimates using reasonable values (i.e. characteristic thicknesses for the enriched radioactive layer of 10 and 20 km and a mantle heat flow of 30 mW/m²) for an exponential depth-decay law of radioactive elements within the granite (Roy et al. 1968) lead to temperature gradients between 27 °C/km and 43 °C/km and temperatures between 135 °C and 215 °C at 5 km depth. The spread in values is obviously large but suggests anyway more favourable conditions for geothermal exploration as compared to most regions of Norway (Pascal et al. 2010). This implies that economic underground temperatures may prevail below all of the municipality of Bergen.

Finally it is important to note that a similar radiometric study carried out in the framework of the “North Sea Crustal Onshore-Offshore Project” (Coop, financed by a consortium of companies including Statoil) in July 2010 has confirmed and extended the results of the present study. As a follow up of the present study and as part of the Coop project, we plan (1) to interpret the newly acquired potential field data and to build a 2D thermal model crossing the Løvstakken Granite and (2) to drill a 1-km deep hole in order to measure temperature gradients and refine our first-order estimates.

4 RADIOMETRIC AND BOREHOLE DATA IN THE OSLO REGION

Christophe Pascal, Torleif Lauritsen, Ole Lutro & Odleiv Olesen

4.1 Airborne radiometrics and natural heat generation

The multi-channel gamma spectrometry data used in the present study were acquired by means of airborne and helicopter surveys from 1981 to 2003 (Smethrust et al. 2006). Most of the area was flown for NGU by Fugro Airborne Surveys Ltd in 2003 in the framework of the GEOS mapping programme. Acquisition and processing details can be found in Fugro Airborne Surveys (2003) and references listed in Smethrust et al. (2006).

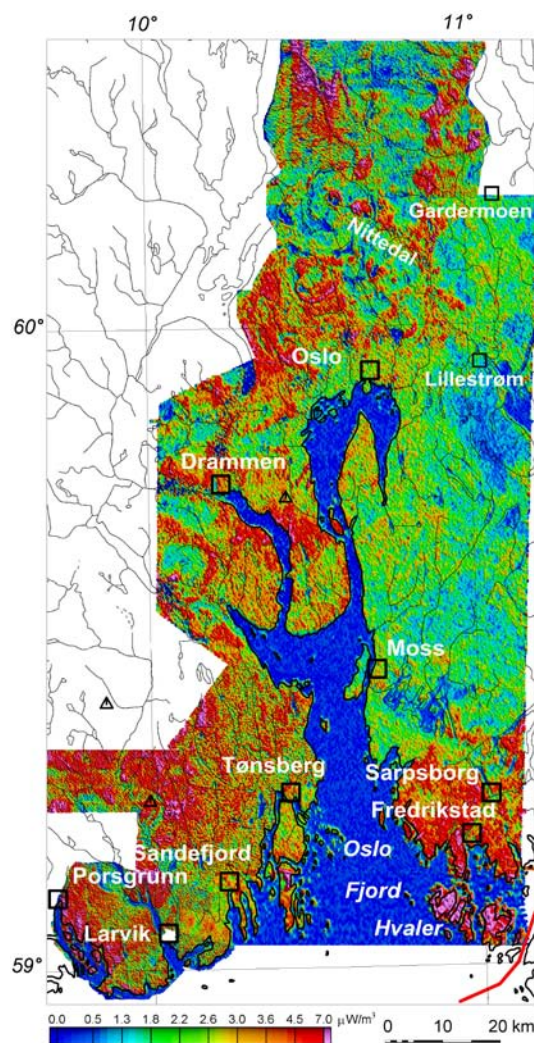


Figure 4.1. Heat generation values calculated from airborne multi-channel gamma spectrometry surveys. Note that the results shown here are not corrected for the attenuation effect of the Quaternary sediments.

Similarly to the ground spectrometry study of the Bergen Region (see Chapter 3), we used the concentrations in uranium, thorium and potassium derived from gamma spectrometry and calculated heat generation values (Fig. 4.1) according to equation (1). In contrast to ground surveys, airborne gamma spectrometry surveys need to be corrected for altitude and its attenuation effects (e.g. Heincke et al. 2009). We find a reasonably good agreement between heat generation values calculated from airborne gamma spectrometry surveys with those calculated from ground surveys (Fig. 4.2), giving us confidence on the accuracy of the altitude corrections made by previous authors (see references in Smethrust et al. 2006). Note, that, with respect to ground surveys, airborne surveys result in lower heat generations, because they average contributions from various radioactive sources. This is well illustrated for the Cambrian alum shales whose radioactivity is extremely high but whose surface exposure is very limited.

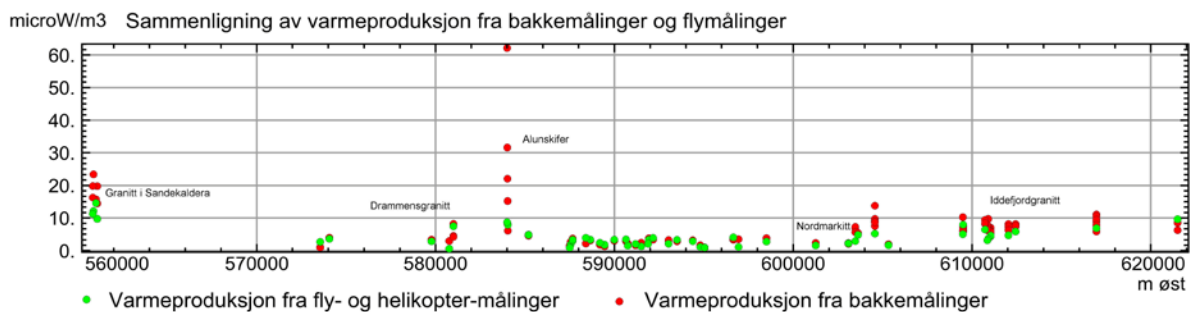


Figure 4.2. Comparison of heat generation values derived from gamma spectrometry airborne surveys with those calculated from gamma spectrometry ground surveys.

Finally, we corrected the heat generation map for the effect of the sedimentary cover. The Quaternary sediments act as a blanket, absorbing gamma particles generated in the rocks they overlay. In order to get a reliable heat generation map of the bedrock, we carefully checked the locations where the bedrock is exposed and filtered out the other areas where it is covered by sediments. We then used the digital bedrock map from Lutro and Nordgulen (2004) and averaged heat generation values over each distinct geological unit. The result of this careful data filtering and subsequent extrapolation is shown in Figure 4.3.

Obvious features of the map are the high heat-producing Permian (e.g. Drammen Granite, Vestfold Igneous Region) and to some extent Precambrian (i.e. Iddefjord Granite) intrusive rocks. The Nordmarka Igneous Complex shows variable, albeit dominantly high, heat generation rates, with typical values between 2 to more than 5 $\mu\text{W}/\text{m}^3$. It is worth noting that for Nordmarka the highest values are associated with exposed granitoids (i.e. depicted in pink tones) that are assumed to be representative of the rocks at depth. The Cambro-Silurian sediments have, in general, moderate contents of radioactive elements and heat generation values of 2 to 2.5 $\mu\text{W}/\text{m}^3$. Low heat generation values characterise the Precambrian basement (shown in blue tones). The Precambrian basement takes, however, surprisingly high heat generation values of 2 to 3.5 $\mu\text{W}/\text{m}^3$ south of Oslo (e.g. at Nesodden) and, presumably, where it exists below the Cambro-Silurian sediments.

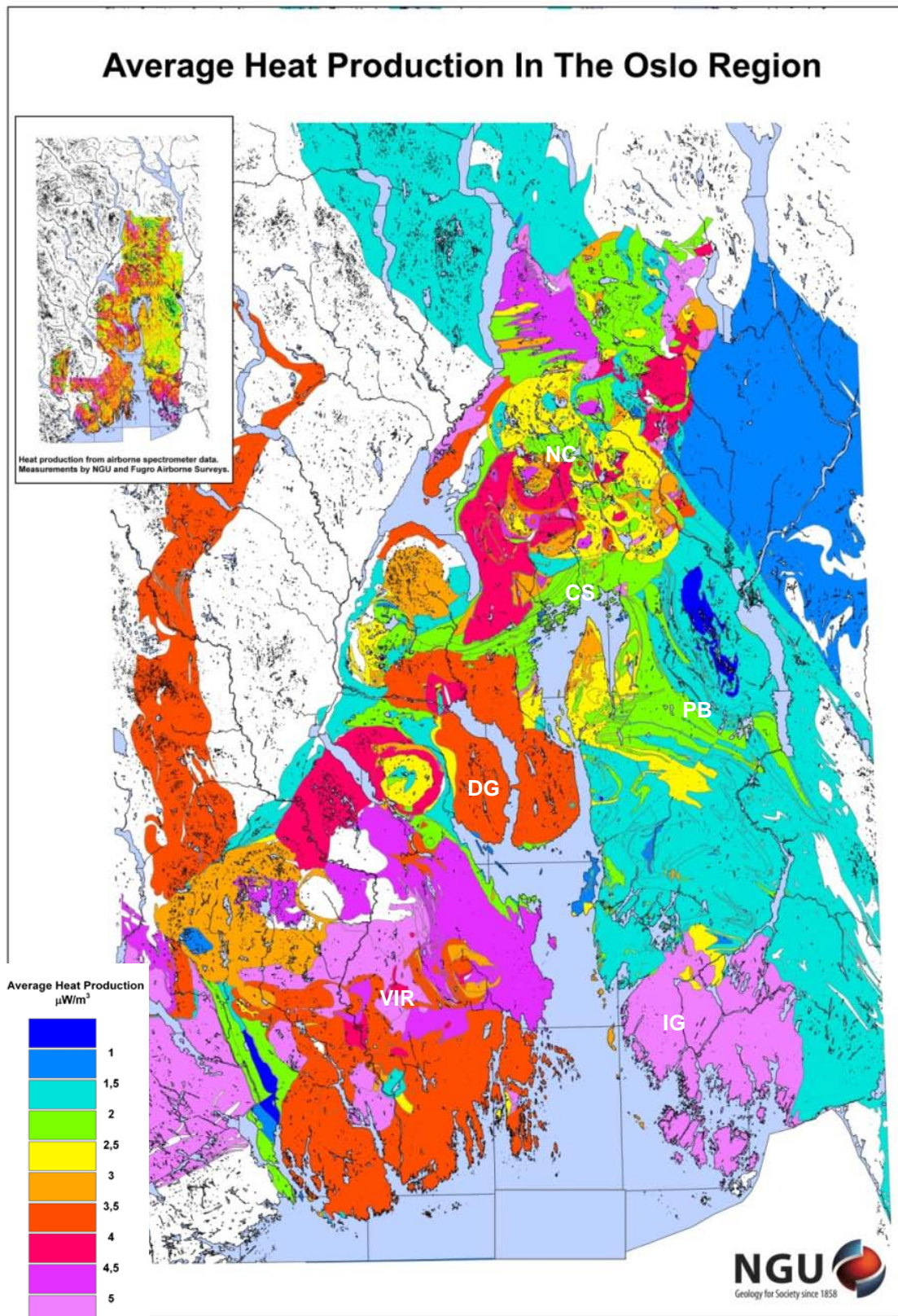


Figure 4.3. Heat generation map of the Oslo Region as derived from airborne gamma spectrometry surveys and corrected for the effect of sedimentary overburden. CS=Cambro-Silurian sediments, DG=Drammen Granite, IG=Iddefjord Granite, VIR=Vestfold Igneous Region, NC=Nordmarka Igneous Complex and PB=Precambrian basement.

4.2 Information gained from the Rikshospitalet, Arnestad and Hamar boreholes

4.2.1 Rikshospitalet borehole

Very little information has been released from the Rikshospitalet boreholes at Gaustad. The boreholes were drilled in 2000-2001 with the aim of exploiting the shallow geothermal resource but the facility has never been completed and the drillholes were abandoned. The deepest borehole (i.e. bh3) was drilled down to ~1500 m total depth and temperatures of 24-27°C (uncorrected and cooled down by the drilling) were measured in the borehole (Musæus et al. 2010). Unfortunately, we do not know the drilled vertical depth and, therefore, it is difficult to estimate temperatures gradients from this piece of very scarce information.

In turn, we recently discovered that the drill cuttings from bh3 were stored at NGU and used them to determine the lithologies penetrated in the well (see Appendix A). The most relevant and unexpected finding is that the Cambro-Silurian sediments rest on Precambrian basement at Gaustad and probably in most places of Oslo.

4.2.2 Arnestad borehole

The Arnestad borehole was drilled with the aim of providing heating to the local school but, again, the facility has never been completed. The drillhole penetrated a pile of Cambro-Silurian sediments down to ~475 m TD and granitic Precambrian basement down to 675 m TD (Elvebakk 2007, Elvebakk personal communication 2009). Slagstad et al. (2009) attempted to calculate heat flow values from the borehole data and came to the conclusion that, even after tentative corrections, the heat flow was erratic and varying from 50 to more than 90 mW/m². Indeed, no core material for thermal conductivity measurements was available for the heat flow determinations of Slagstad et al. (2009). We figured out a second problem. Borehole deviation was only known down to ~475 m TD (i.e. ~450 m TVD), rendering difficult any determination of the temperature gradient below that depth.

We tried to improve the heat flow determinations of Slagstad et al. (2009) by means of sampling rock material in Arnestad for thermal conductivity measurements. Unfortunately, the rocks (mainly shales) turned to be very friable and extremely difficult to sample. An additional limitation came from the complex geometry of the folded and thrust rocks that were penetrated in the borehole, making their comparison with their counterparts exposed at the surface a hopeless task in the absence of core material.

Two useful informations for the thermal modelling can, nevertheless, be extracted. Firstly, the basement underlying the Cambro-Silurian sediments in Arnestad is Precambrian in age and not a highly radioactive Permian granitoid (i.e. Drammen Granite, exposed a few kilometres west of Arnestad). Secondly, the temperature gradient in the sediments, measured well after the drilling, falls in the range between 25 and 30°C/km, suggesting that temperatures about 30-35°C should normally prevail below 1 km-thick Cambro-Silurian rocks. Note that this

estimate is, at first glance, in reasonable agreement with the temperatures derived from the Rikshospitalet bh3 borehole.

4.2.3 Hamar borehole

As stated above, it turned to be difficult to sample fresh rock in order to increase our database of thermal conductivity measurements on the Cambro-Silurian sediments. For the modelling, we used the measurements made on core material from the Hamar borehole. The Hamar borehole was drilled and completely cored in the framework of the Kontiki project in 2005 (Olesen et al. 2007). It penetrated a thick layer of Cambro-Silurian sediments down to ~800 m (Fig. 4.4), representative of the main lithologies involved in this type of rocks in the Oslo Region. Ninety-eight samples were measured for thermal conductivity (Midttømme et al. 2007). The minimum and maximum measured values are 1.4 W/(m.K) and 4.5 W/(m.K) respectively. A statistical analysis of the thermal conductivity measurements results in a median and mean value equal to 2.2 W/(m.K). Bearing in mind that the black shales are overrepresented in the Hamar borehole and that their respective thermal conductivities are lower than for the other sediments, this previous study constrains the range of values needed for the thermal modelling.

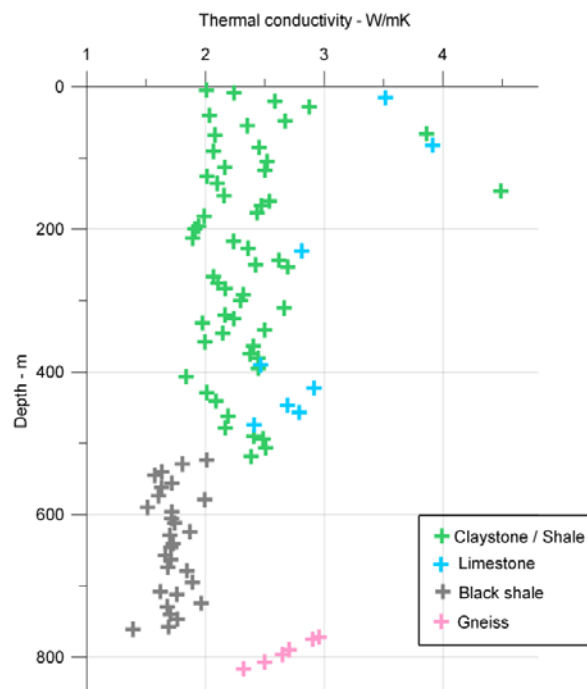


Figure 4.4. Thermal conductivities measured on 98 samples of core material from the Hamar drillhole (after Midttømme et al. 2007).

4.3 Conclusions

The purpose of the present chapter was to gather all information available to constrain the 3D thermal model. The informations can be divided in two classes: structural and geothermal. The two deep boreholes drilled in the area of interest (i.e. Rikshospitalet bh3 and Arnestad boreholes) penetrated the Precambrian basement below the Cambro-Silurian sediments. It suggests that, in general, the Cambro-Silurian sediments rest directly on the basement and not on Permian intrusions.

The geothermal data at hand (i.e. airborne radiometric data and temperatures and thermal conductivities derived from the two drillholes) show that:

- the Nordmarka Igneous Complex has high but variable heat generation rates ranging from 2 to more than 5 $\mu\text{W}/\text{m}^3$, however, outcropping granitic bodies suggest that heat generation at depth is higher than the average measured at the surface;
- the Cambro-Silurian sediments have moderate generation rates (i.e. 2 to 2.5 $\mu\text{W}/\text{m}^3$) and relatively low thermal conductivities (i.e. mainly in the range 2 to 2.5 $\text{W}/(\text{m}\cdot\text{K})$);
- the Precambrian basement near and presumably below Oslo and Asker has relatively high generation rates (i.e. 2 to 3.5 $\mu\text{W}/\text{m}^3$);
- temperatures in the range 30-35°C are expected below ~1 km of Cambro-Silurian sediments.

5 3D CRUSTAL MODELLING (OSLO-ASKER)

Jörg Ebbing, Christophe Pascal, Marianne Aarseth, Torleif Lauritsen & Odleiv Olesen*

The integrated interpretation of gravity and magnetic field data constrained by petrophysical data and surface geology reveals the location of magmatic intrusions below the Oslo Graben and provides an estimate of the thickness of the Cambro-Silurian sedimentary sequences.

We use a 3D model described in detail by Ebbing et al. (2007), which is refined with respect to the detailed surface petrophysics and with special attention to the thickness of the Cambro-Silurian sequences.

5.1 Data

5.1.1 Petrophysics

More than 2,700 rock samples, collected during geological mapping and geophysical studies, have been measured with respect to density, susceptibility and remanence. The data are stored in NGUs petrophysical database (Olesen et al. 1993). The data are averaged for geological units according to the geological map of Lutro and Nordgulen (2004). Non-representative samples were removed from the dataset before map production.

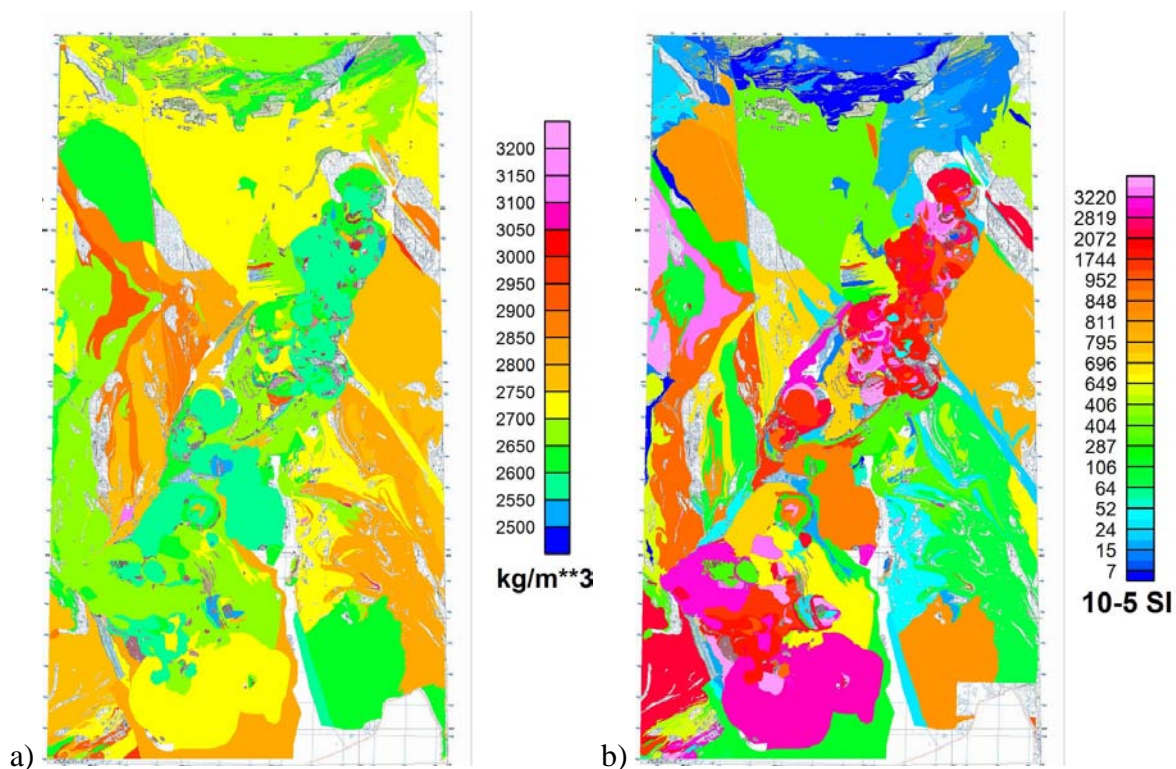


Figure 5.1. a) Average density and b) average susceptibility of bedrock samples within each geological unit of the Oslo Region bedrock map (Lutro and Nordgulen 2004).

The density map shows rather homogeneous densities within the Oslo Graben (Figure 5.1a), whereas some larger changes are observed to the east and in the western border. Measured densities in the Kongsberg and Bamble sectors fall around 2850 kg/m^3 , higher than those in the Precambrian rocks of the Telemark sector and the Østfold Complex to the west and east, respectively. The Cambro-Silurian sedimentary rocks have an average density of 2700 kg/m^3 , higher than surface magmatic rocks ($\sim 2600 \text{ kg/m}^3$).

Magnetic susceptibility in the Oslo Graben ranges from 0.0001 SI to 0.1 SI depending on rock material, but also with spatial variations (Figure 5.1b). The southern Oslo Graben (the Vestfold Igneous Region, Fig. 5.2) is marked by high susceptibilities, generally >0.02 SI. These susceptibilities are mainly related to larvikite intrusions. The central part of the Oslo Graben shows moderate magnetic susceptibilities associated with the Drammen Granite. The northern part (the area of the Nordmarka Igneous Complex) features high-magnetic material at the surface and magnetic susceptibilities are again generally >0.02 SI. The uneven distribution of high-magnetic rocks thus indicates a division of the Oslo Graben into three parts: high-magnetic southern and northern parts and a less magnetic area in between. In the surrounding areas of the Oslo Graben the rocks show only low magnetization. The Cambro-Silurian sedimentary rocks show susceptibility values similar to the bedrock surrounding the Oslo Graben, in the order of 0.005-0.01 SI, which makes them difficult to distinguish. These observations are clearly important when modelling the magnetic field.

5.1.2 Gravity data

The complete Bouguer anomaly is presented in Figure 5.2a and a snapshot of it from the area under scope here in Figure 5.3. In the area of the Oslo Rift Region, more than 12,000 gravity points exist. In the northern Oslo Rift, across the Oslo Graben, a broad Bouguer gravity high is present with amplitudes up to 50 mGal, whilst the surrounding areas show values down to -80 mGal on the western side and -20 mGal on the eastern side. On a profile this is expressed by a steep, westward-facing gradient partly located to the west of the rift, and a much gentler eastern gradient (Ebbing et al. 2007). The irregular shape of the anomaly and its offset to the rift axis points to an additional source of the anomaly in addition to the volcanic rocks observed at the surface.

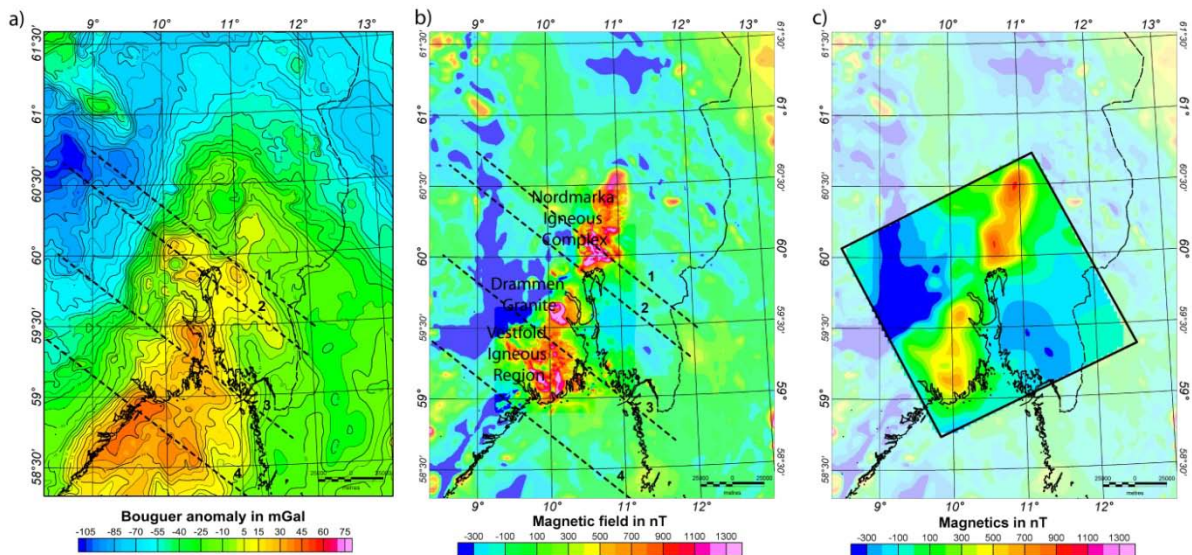


Figure 5.2. Gravity and magnetic fields of the Oslo Rift Region. a) Bouguer anomaly map. The data compilation is based on data sets collected by NGU, SGU, the universities of Oslo and Aarhus, ExxonMobil, Statoil and the Norwegian Mapping Authority (Skilbrei et al. 2000). b) High-resolution aeromagnetic survey merged with adjacent low-altitude, draped aeromagnetic survey flown in 1973 (Olesen et al. 1997, Korhonen et al. 2002). c) The square indicates the data of the high altitude aeromagnetic survey (3000 m flight altitude) as part of the Norwegian Geotraverse project (Aalstad et al. 1977, Heier 1977). Surrounding low-altitude data are shown in transparent colours.

5.1.3 Magnetic data

The coverage of magnetic field data in the Oslo Region is unique in Norway and allows for using simultaneously surveys recorded at two different flight altitudes (Figures 5.2b, 5.2c and 5.3). The advantage of having magnetic datasets from two different altitudes is that the decay of the magnetic field with height for possible source bodies can be analyzed using real data. The attenuation of the magnetic fields with distance from the geological source is dependent on structure. Therefore, if the magnetic data are measured at two observation levels, one can use this difference to model the geometry or source thickness. Subsequently, models that fit data at different levels 'simultaneously' can be constructed.

Low-altitude aeromagnetic data

A low-altitude aeromagnetic survey was flown in 2003 as part of the GEOS project, with a line spacing of 250 m and a flight altitude of 50 m over the central Oslo Region. For the area adjacent to the new high-resolution dataset, we merged our data with another, low-altitude, draped aeromagnetic survey flown in 1973, with 400-500 m line spacing and mean height above terrain of 150 m (Olesen et al. 1997, Korhonen et al. 2002), which has been combined with the modern, high-sensitivity survey located above the Oslo Graben (Figure 5.2b).

High-altitude aeromagnetic data

A high-altitude aeromagnetic survey was flown already in 1970 as part of the Norwegian Geotraverse Project (Aalstad et al. 1977, Heier 1977). Hand-contoured maps have been digitized to produce the grid in Figure 5.2c. The constant flight altitude of 3400 m above sea level and a line spacing of 3 km were chosen to reduce the effect of varying terrain and to map regional-scale features. The flight altitude and line spacing give an unambiguous coverage, with the line spacing less than the altitude throughout the area.

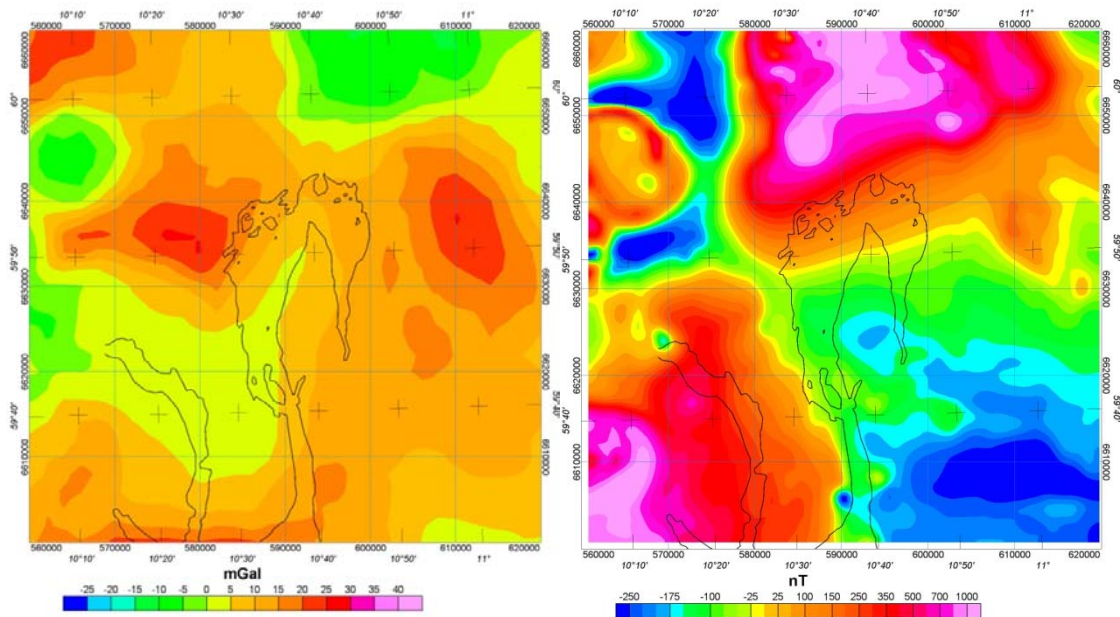


Figure 5.3. Local maps of Bouguer (left panel) and magnetic (right panel) anomalies. Note (1) the modest amplitudes in the gravity field, making its use difficult for modelling their respective density sources and (2) the smooth magnetic gradient south of the Nordmarka Igneous Complex, suggesting extension of the complex below Oslo downtown and the Oslofjord.

5.1.4 Seismic data

In contrast to the well-defined potential field and petrophysical datasets, the knowledge about the structure of the Oslo Graben from seismic experiments is rather sparse. In the area of the Oslo Graben only two seismic refraction lines were available at the start of the present project (Tryti and Sellevoll 1977). Their interpretation shows a high-velocity lower crust below the Oslo Rift ($V_p \sim 7.1$ km/s), but for the shallower crustal levels the refraction experiments could not provide details about the crustal geometry. Existing seismic profiles from regions adjacent to the Oslo Graben also feature a high-velocity layer at the base of the crust ($V_p > 7$ km/s e.g. Kinck et al. 1993, Korsman et al. 1999).

5.2 Potential field anomalies and surface geology

Comparison between surface geology and potential field anomalies allow for a first-order characterisation of the possible sources. Gravity and magnetic anomalies show, however, a signal reflecting the superposition of all relevant sources. This means that the anomalies show a signal related the entire crustal structure, and not limited to the geology visible at the surface.

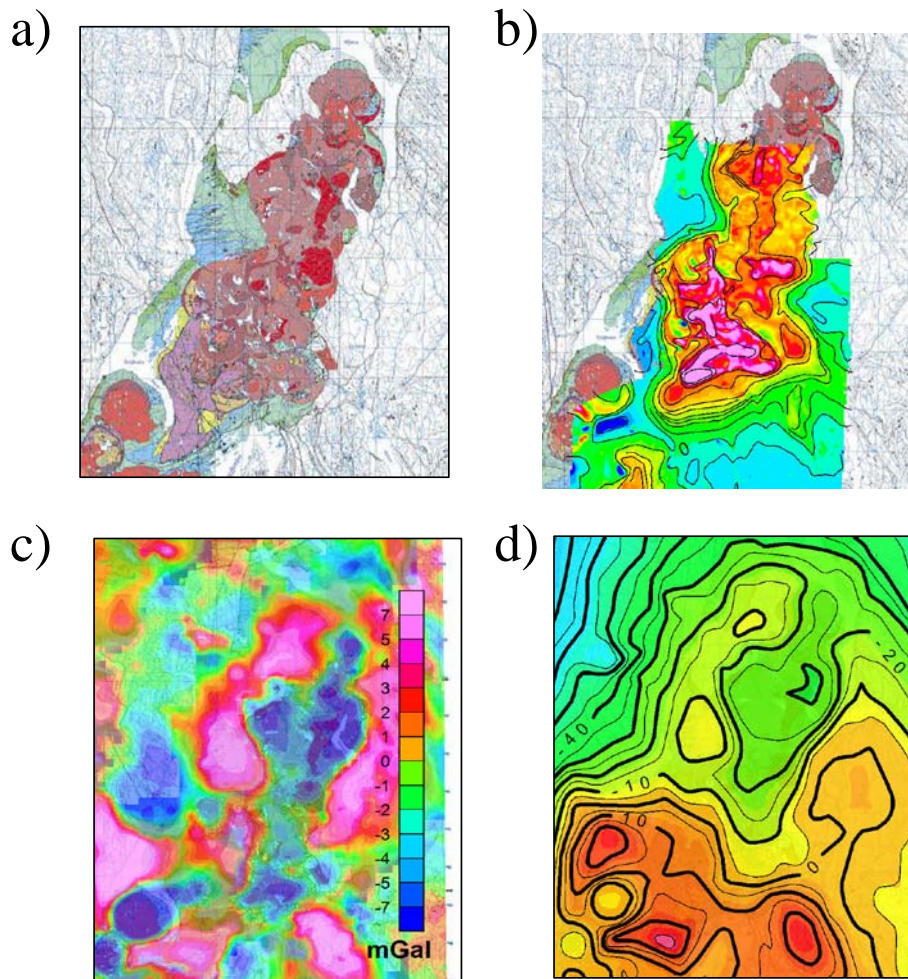


Figure 5.4. Nordmarka Igneous Complex and surroundings. a) snapshot of the geological map of the Oslo Graben (Lutro and Nordgulen 2004), b) high-resolution aeromagnetic anomaly (colour scale as in Figure 5.2b), c) high-pass filtered Bouguer anomaly (cut-off wavelength 40km), d) Bouguer anomaly (colour scale as in Figure 5.2a).

Figure 5.4 shows the geological map of the Nordmarka Igneous Complex and surroundings. The magnetic anomaly correlates strongly with the distribution of magmatic rocks, and shows a sharp gradient to the surroundings, except at its southern edge. The magmatic rocks with their high susceptibility dominate the magnetic anomaly with positive values up to 1500 nT. In the west the Cambro-Silurian domain correlates with an area of low magnetic amplitudes,

while the southeastern part is difficult to identify due to the gradient associated with the southern edge of the Nordmarka Igneous Complex.

The Bouguer gravity anomaly appears to show a relative gravity high surrounding the Nordmarka Igneous Complex. As the Bouguer anomaly is dominated by long-wavelength signals from the crust-mantle boundary and the lower crust, we apply a high-pass wavelength filter with a cut-off wavelength of 40 km. This filter enhances the gravity signal from shallower sources. The filtered anomaly (Figure 5.4c) enhances the relative gravity high surrounding the Nordmarka Igneous Complex and shows some correlation with the location of Cambro-Silurian sedimentary rocks on the geological map (compare Figure 5.4a and c), although the gravity high is not limited to the area where Cambro-Silurian rocks are present.

5.3 3D modelling

All the different datasets (two aeromagnetic fields flown at two different altitudes, the gravimetric field, as well as petrophysical data) are integrated into one model that fulfills all observed data sets. In total, the 3D model is constructed by vertical sections with a 15 km spacing between the planes outside the Oslo Graben, to 3 km within the Oslo Graben. While special emphasis was given initially to the resolution of the volcanic and plutonic structures of the Oslo Graben in the construction of the model, now the emphasis was given to a reliable estimate of the Cambro-Silurian sequences overlying the plutonic sequences.

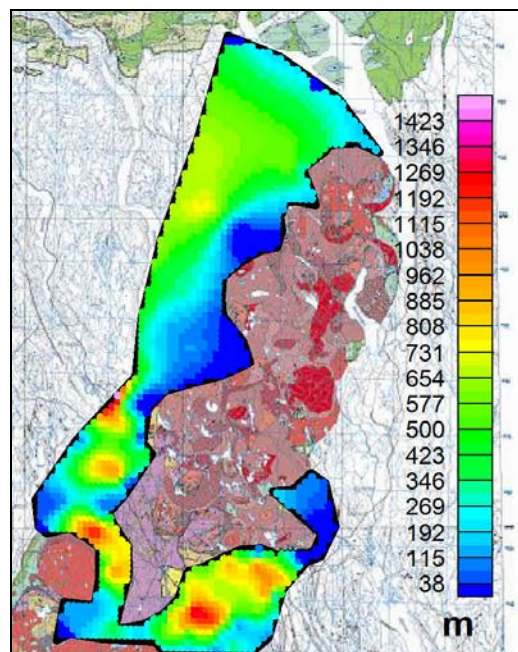


Figure 5.5. Thickness of Cambro-Silurian sedimentary rocks from the 3D model.

First, the available information on surface geology, petrophysical measurements and seismics was used in order to constrain a density model of the Oslo Rift. The 3D density model of the Oslo Rift explains the regional shape of the Bouguer anomaly as a combined effect of crustal thinning and the presence of a transcrustal ramp related to a mid-crustal layer that reaches the surface in the Kongsberg and Bamble Complexes (Ebbing et al. 2005, 2007). This is in agreement with the observed high densities of the over-thrusted high-grade and high-density Kongsberg and Bamble Complexes and the asymmetric shape of the gravity high (Ebbing et al. 2005, 2007).

The two major magnetic anomalies in the Oslo Graben are located above the Nordmarka Igneous Complex and the Vestfold Igneous Region. The rocks at the surface are heterogeneous and feature a variety of igneous rocks (e.g. syenite, granite, basalt), which are included with their magnetic properties in the model.

The focus was given on providing an estimate of the thickness of the Cambro-Silurian sedimentary rocks. One pinpoint for the model is given by the bh3 borehole at the Rikshospitalet in Gaustad (c. 115 m a.s.l.), where Precambrian gneisses were encountered at 880 m TD (alas without correction for deviation, see Chapter 4 and Appendix A). In the 3D model, the Cambro-Silurian is modelled from the surface to depth. The extension at the surface is taken from the geological map of the Oslo Region (Lutro and Nordgulen 2004). Figure 5.5 shows the thickness of the Cambro-Silurian sedimentary rocks as derived from the 3D model. The modelling suggests a relatively thin layer of sediments with thicknesses less than 1 km in general.

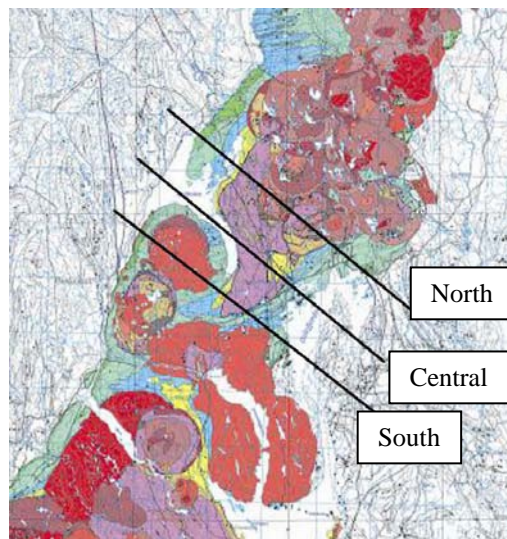


Figure 5.6. Location of the three NW-SE trending cross-sections presented in Figures 5.7 to 5.9 below. Geological map of the Oslo Graben from Lutro and Nordgulen (2004).

In order to show the main structural characteristics of the crust as derived from the 3D model in the area of interest, we present three NW-SE trending cross-sections (Figure 5.6).

Section South

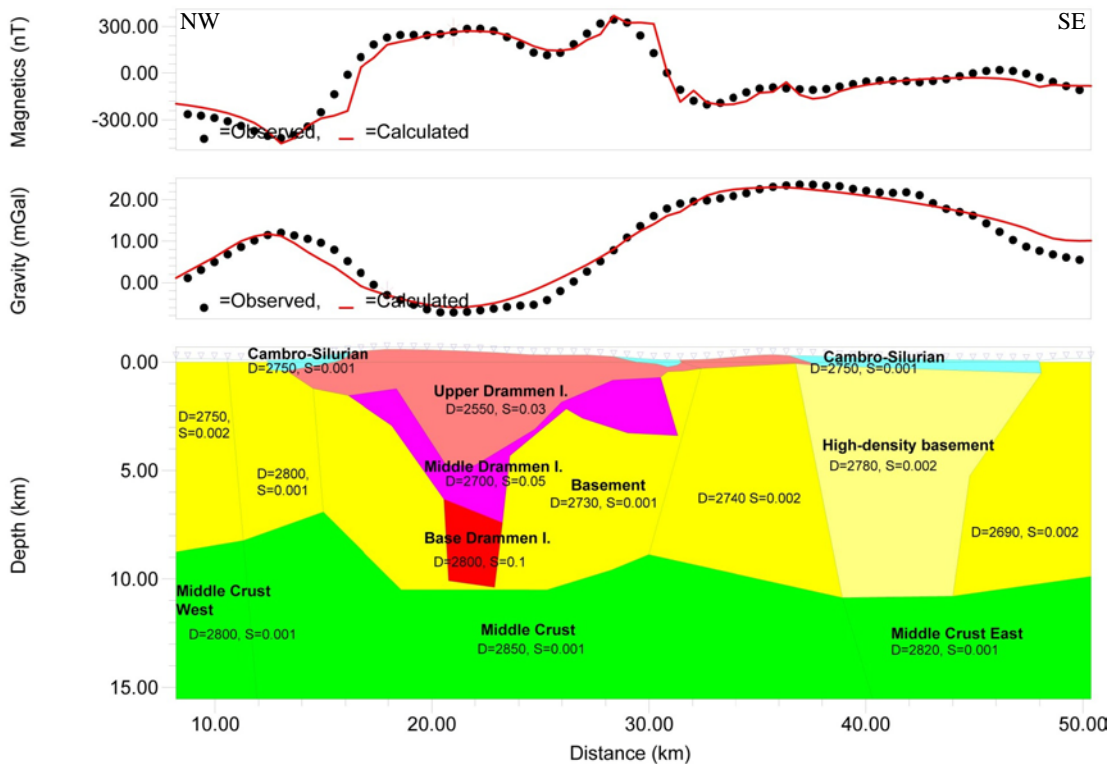


Figure 5.7. Section South of the 3D crustal model crossing the Drammen Granite. Note the sharp magnetic gradient at the SE boundary of the granite indicating that it does not extend farther to the east, as also shown by the lithologies encountered in the Arnestad borehole (see Chapter 4).

The southernmost section crosses the Drammen Granite (Figure 5.7). The model suggests that the Drammen Granite has a mushroom shape with relatively thin edges. Furthermore, in order to reproduce the sharp decay in the magnetic field at the eastern edge of the granite, we assumed that its boundary is equally sharp and that the granite does not extend farther to the east below the Cambro-Silurian sediments. This assumption is also in agreement with the lithologies penetrated in the Arnestad borehole, where Precambrian basement was identified at ~450 m TVD (see Chapter 4).

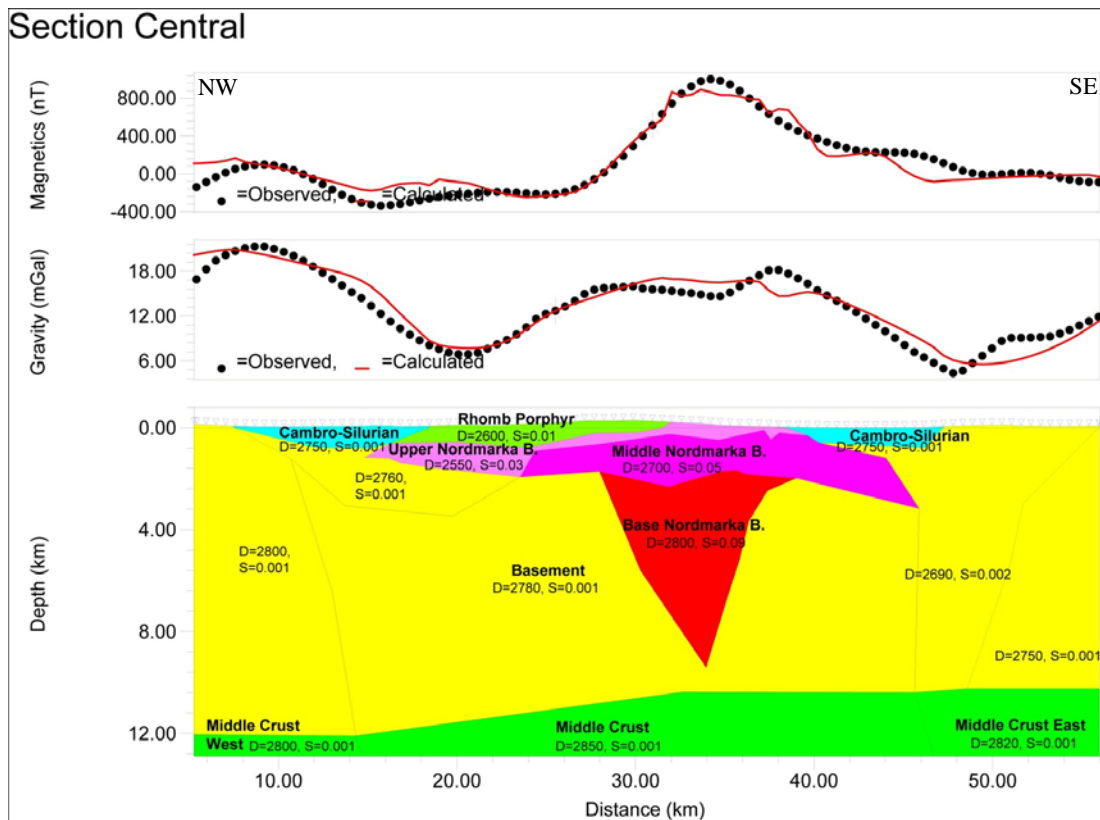


Figure 5.8. Section Central of the 3D crustal model crossing the southern edge of the Nordmarka Igneous Complex. Note the smooth magnetic gradient at the SE boundary of the granite indicating its extension to the east. A thin layer of Precambrian basement between the Cambro-Silurian sediments and the Nordmarka Granite has been modelled in order to account for the observed lithologies in the Rikshospitalet borehole.

The central section crosses the southwestern edge of the Nordmarka complex (Fig. 5.6 and 5.8). The smooth decay of the magnetic anomaly at its southeastern edge indicates that its associated plutonic rocks extend farther to the SE below the Cambro-Silurian sediments (Fig. 5.8). A thin layer of Precambrian basement has, nevertheless, been added between the pluton and the Cambro-Silurian sediments in order to account for the observed lithologies in the Rikshospitalet bh3 borehole (see Chapter 4). Noteworthy, the shape of the modelled contact between Permian rhomb porphyry lava flows and Cambro-Silurian sediments is nonsense from the geological point of view. This kind of mistakes have been corrected while building the 3D thermal model presented in Chapter 6.

Section North

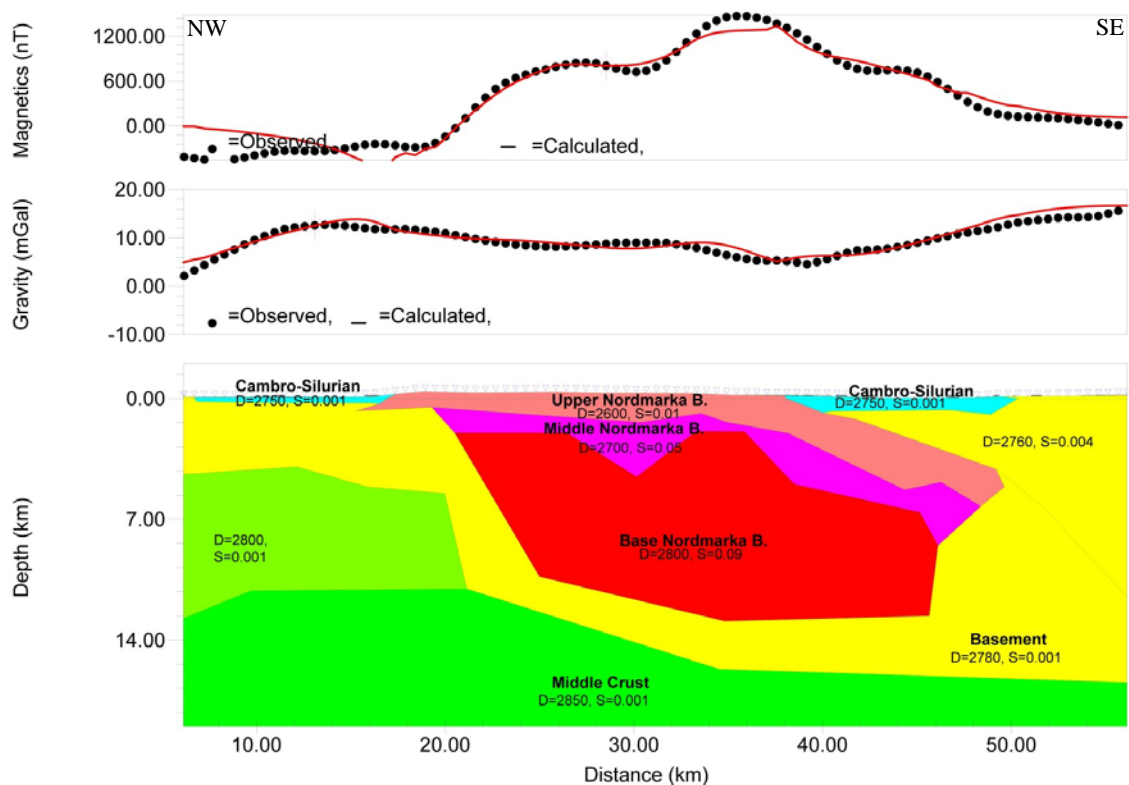


Figure 5.9. Section North of the 3D crustal model crossing the middle part of the Nordmarka Igneous Complex. Note the smooth magnetic gradient at the SE boundary of the granite indicating its extension to the east. A thin layer of Precambrian basement between the Cambro-Silurian sediments and the Nordmarka Igneous Complex has been modelled in order to account for the observed lithologies in the Rikshospitalet borehole.

The northern section (Figs. 5.6 and 5.9) crosses the middle part of the Nordmarka complex and presents characteristics similar to those of the central section (i.e. smooth decay of magnetic anomalies at the SE edge of the complex and involvement of a Precambrian basement layer between plutonic rocks and Cambro-Silurian sediments). However, the 3D model suggests a much thicker batholith, as compared to the previous profile, extending to depths down to 14 km.

5.4 Conclusions

The small contrasts in density of the rocks present in the area of interest (i.e. Oslo-Asker) imply modest Bouguer gravity anomalies and render the 3D model somewhat uncertain when attempting to model at typical length scales of tens of kilometres. The magnetic field shows much more pronounced variations and allows for strengthening our results. Ideally, potential field methods gain in robustness when supplemented with seismic data and information from drillholes, both data sources being scarce in the Oslo Region.

Nonetheless, a few robust conclusions, mainly supported by the modelling of the magnetic anomalies and information from the two drillholes known to have penetrated the basement, can be derived from our modelling study:

- the Nordmarka Igneous Complex extends farther to the south below Oslo and the Inner Oslofjord;
- the Drammen Granite has a sharp and steep eastern boundary;
- the Cambro-Silurian sediments appear to rest on the Precambrian basement;
- the Nordmarka Igneous Complex appears to be thick (more than 10 km in its middle part).

More uncertain remain the thickness estimates for the Cambro-Silurian sediments mainly because of their poor contrast in density and magnetic susceptibility with the underlying Precambrian basement. The Rikshospitalet and Arnestad drillholes suggest thicknesses less than one km, that we used to constrain the modelling, but we cannot exclude that the sediments are locally much thicker elsewhere in the modelled domain.

6 3D THERMAL MODELLING (OLSO-ASKER)

Christophe Pascal

6.1 Introduction

This chapter presents the 3D thermal model built on the basis of the information summarised in the two previous chapters. The main goal of the thermal modelling was to quantify underground temperatures in the Oslo-Asker area. The results of the modelling are then used to discuss the geothermal potential of the area.

6.2 Modelling strategy

The computations were carried out using the commercial software FLAC3D 4.00 (www.itascacg.com/flac3d). FLAC3D is a modelling code designed to calculate large deformations and involves different types of rheologies but can also be used for steady-state or transient thermal computations. The code utilises an explicit finite difference formulation. In the present case, we used FLAC3D to solve the three dimensional form of the steady-state heat equation:

$$q = -k \cdot \frac{\partial T}{\partial z} \quad (2)$$

where q is heat flow, k thermal conductivity, T temperature and z depth (positive downwards). More detailed mathematical aspects can be found in e.g. Haenel et al. (1988).

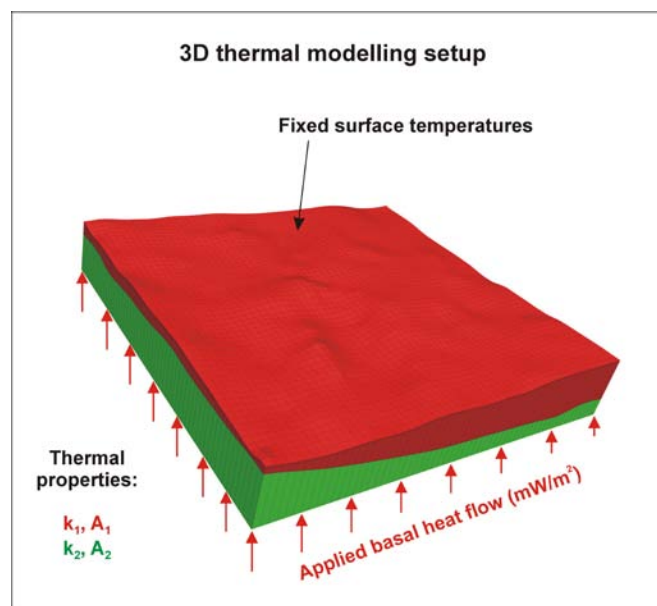


Figure 6.1. Modelling setup used in the present study. Surface temperatures and basal heat flow are applied and each rock unit has its own thermal properties (i.e. A , heat generation and k , thermal conductivity).

Table 6.1. Ranges of thermal parameters used to constrain the modelling (see Chapter 4).

	Thermal conductivity (W/K.m)	Heat generation ($\mu\text{W}/\text{m}^3$)
Sediments	2.0-2.5	2.0-2.5
Precambrian basement	3	1-2
Upper Nordmarka	3	3- >5
Middle Nordmarka	3	3- >5
Lower Nordmarka	3	1-3

Equation (2) is solved considering the presence of internal sources of heat (i.e. heat generation by decay of radioactive elements in rocks) and considering the set of boundary conditions given in Figure 6.1. A fixed surface temperature of 5°C, corresponding to present-day annual averages for air temperature in the Oslo Region (www.senorge.no), and a basal heat flow in the range 30 to 40 mW/m² are applied to the model. The basal heat flow was estimated by us based on a priori regional crustal compositions and the heat flow estimates from Pascal et al. (2010). Heat generation rates were estimated according to the results of the airborne radiometric survey presented in Chapter 4 (Fig. 4.3, Table 6.1). We set a standard value of 3 W/(K.m) (Clauser and Huengens 1995) for the thermal conductivity of the Precambrian basement and the Nordmarka Igneous Complex and used the thermal conductivity measurements on core material from the Hamar drillhole (Chapter 4, Fig. 4.4) to estimate a range of values for the sediments (Table 6.1).

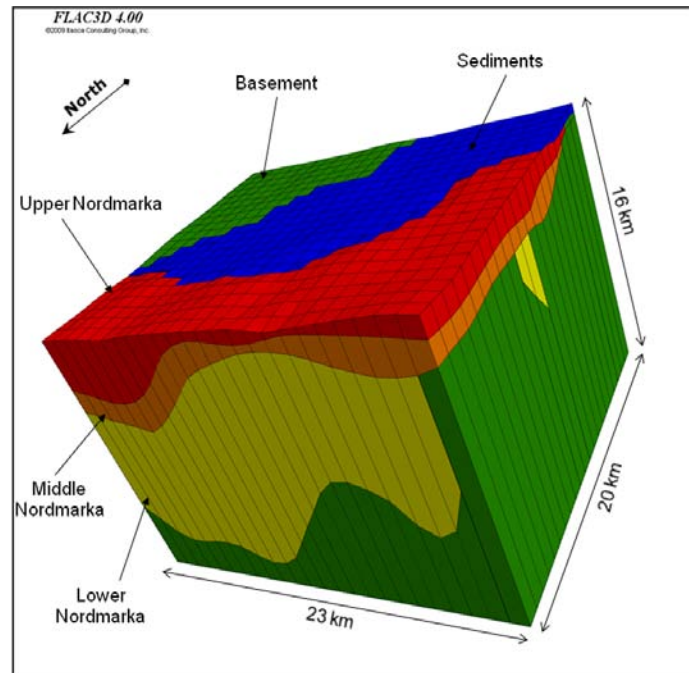


Figure 6.2. View of the structure of the 3D thermal model. Oslo downtown is located in the centre of the top surface.

We built the geometry of the 3D thermal model according to the results of the crustal modelling presented in Chapter 5 (Figs. 6.2, 6.3). The dimensions of the model and the rock units introduced in it are shown in Figure 6.2. The 3D model involves ~2700 gridpoints and ~2000 zones with, in general, an irregular brick shape, allowing for a good balance between model accuracy and computation time.

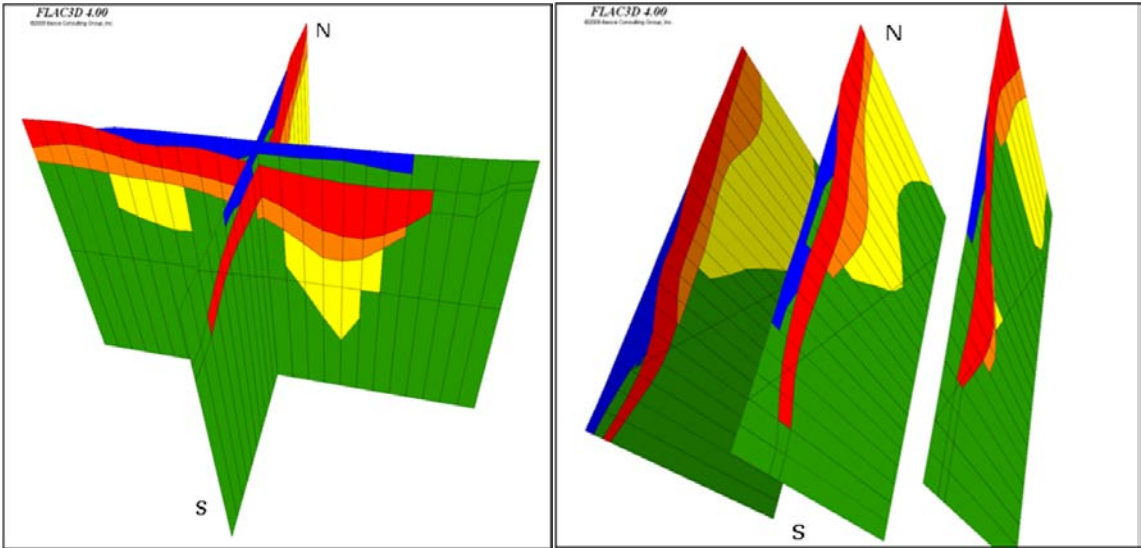


Figure 6.3. 2D slices across the 3D model with view due to the north. Colour code is similar to Figure 6.2.

6.3 Modelling results

We modelled three different scenarios (Table 6.2). The “Optimistic” and “Pessimistic” scenarios represent end-member cases based on the range of thermal parameters given in Table 6.1.

Table 6.2. Thermal parameters used for the three modelled cases. Heat flow values of 30, 40 and 35 mW/m² are applied to the “Optimistic”, “Pessimistic” and “Preferred” scenarios, respectively.

	Thermal conductivity (W/K.m)			Heat generation (μW/m ³)		
	Optimistic	Pessimistic	Preferred	Optimistic	Pessimistic	Preferred
Sediments	2	2.5	2.5	2.5	2.5	2.5
Prec. basement	3	3	3	2	1	2
Upper Nordmarka	3	3	3	6	3	4
Middle Nordmarka	3	3	3	6	3	4
Lower Nordmarka	3	3	3	3	1	2

The “Optimistic” scenario involves the lowest thermal conductivity for the sediments and the highest heat generation values, in particular, for the basement and the two upper layers of the Nordmarka Igneous Complex, whereas maximum sediment conductivity and minimum heat generations are applied for the “Pessimistic” scenario. The “Preferred” scenario represents an intermediate case (Table 6.2). Note that the applied basal heat flow also differs from one scenario to the other: 30 mW/m² for the “Pessimistic” scenario, 35 mW/m² for the “Preferred” one and 40 mW/m² for the “Optimistic” scenario.

Figure 6.4. shows the modelled isotherms up to 100°C along a vertical section crossing the centre of the model and for the two end-member scenarios (i.e. “Optimistic” and “Pessimistic”). The depth of the 100°C isotherm increases from ~3.5 km for the “Optimistic” scenario to ~6 km for the “Pessimistic” one, illustrating how much our calculations are sensitive to the input parameters and their respective uncertainties.

For both modelled scenarios, we note an upward convex shape of the isotherms with an apex located by the middle part of the profile. This local rise in temperatures is the natural result of the thickening of the layers containing the most radiogenic rocks in the model (i.e. Upper + Middle Nordmarka), themselves blanketed by the low conductive sediments. However the modelled isotherms remain relatively flat even in the case of the “Optimistic” scenario, despite significant variations in rock properties. This is in particular true when increasing depth, the structure of the modelled crust becoming more uniform and consequently, lateral variations in temperature less pronounced.

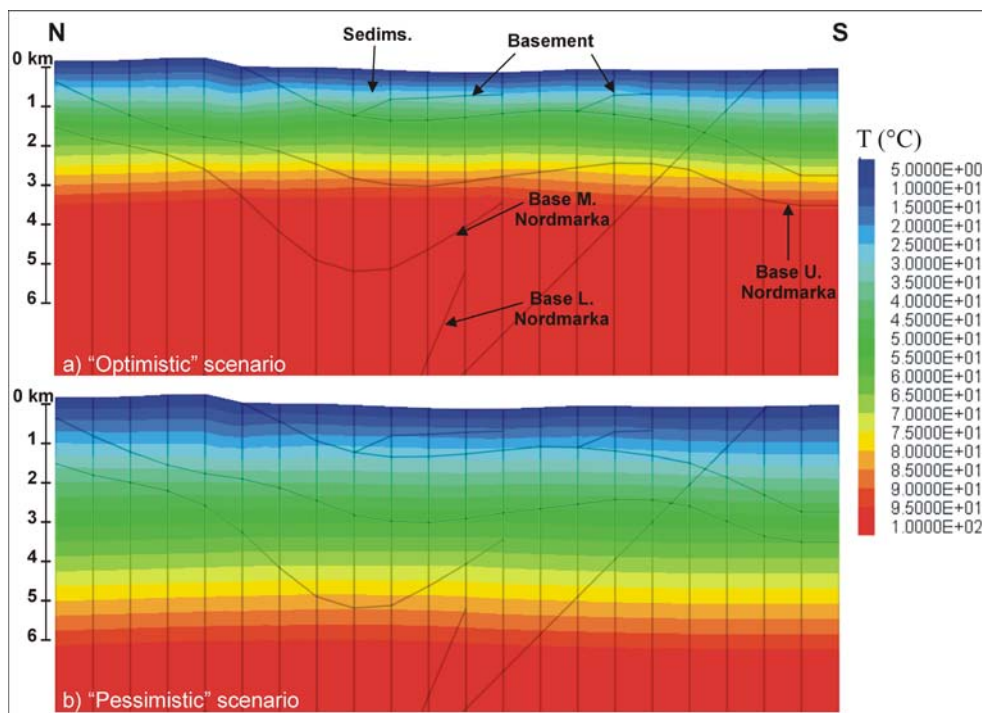


Figure 6.4. Modelled temperature distributions for the “Optimistic” and “Pessimistic” scenarios (see Table 6.2) along the central cross-section shown in Figure 6.3. Note the dramatic change in depth of the 100°C isotherm and, for both scenarios, the almost horizontal isotherms (no vertical exaggeration).

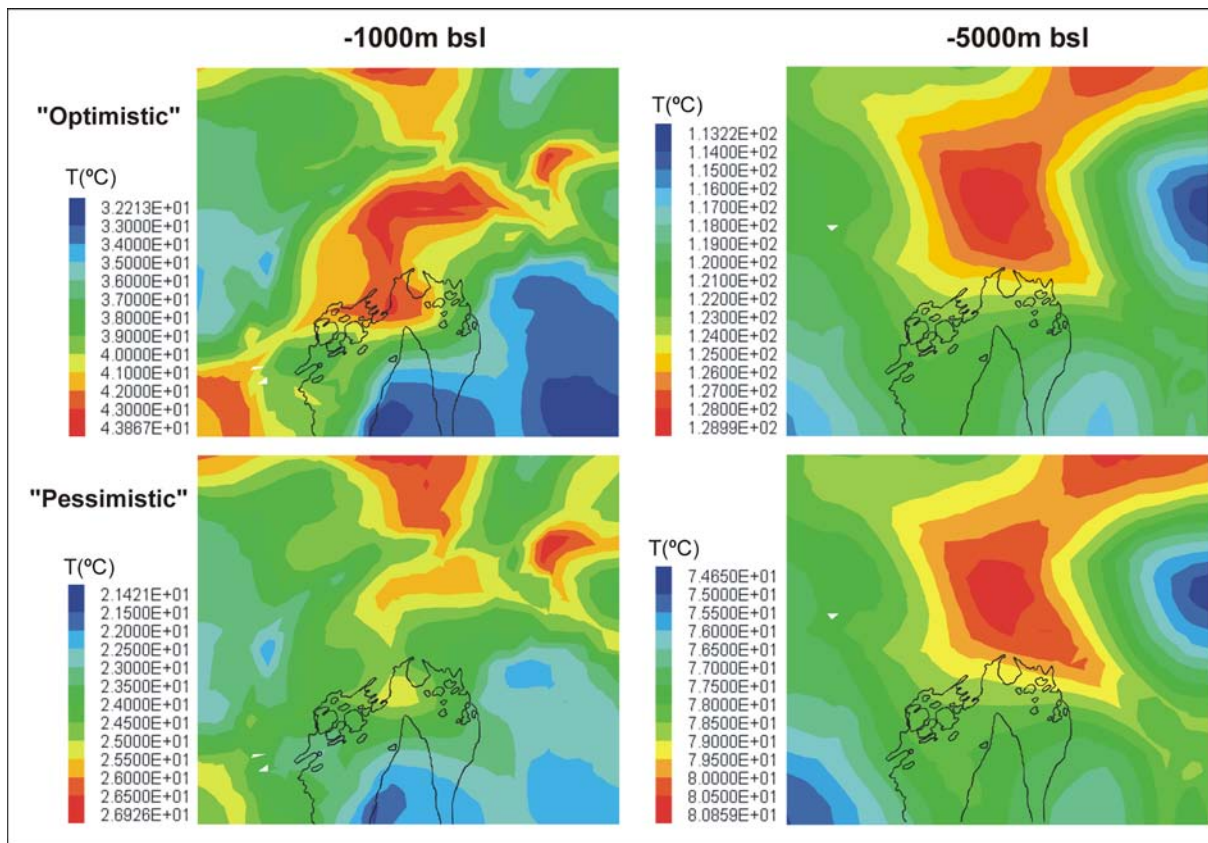


Figure 6.5. Modelled temperature distributions for the “Optimistic” and “Pessimistic” scenarios (see Table 6.2) at 1 and 5 kilometres depth below sea-level. The apparent “positive” anomaly seen below the northern edge of the model at 1 km bsl is partly caused by the altitude of the Nordmarka Plateau (i.e. depth below ground surface is actually 1300-1400 m there).

The modelled temperature slices shown in Figure 6.5 support this latter statement. For example, variations between the minimum predicted temperature and the maximum one amount to ~37% at 1 km depth bsl but only to 14% at 5 km depth bsl, in the case of the “Optimistic” scenario. As expected, temperature variations at corresponding depths are even lower in the case of the “Pessimistic” scenario (i.e. 28% and 8% at 1 and 5 km depth bsl, respectively). This is because variations in both thermal conductivity and heat generation between the different rock units are less significant here than for the previous modelled scenario (i.e. this modelled case is more uniform in properties than the previous one). Nevertheless, the most important lesson we learn from the present modelling exercise is that, in our studied area, careful targeting of the drilling site is more important for the shallow geothermal resource than for the deeper one.

We note that the temperature patterns (but not the temperatures themselves) are very similar for the two modelled cases at equivalent depths (Fig. 6.5). At 1 km depth bsl, the temperature highs are mainly located below Oslo downtown, Bærum and southwest of Asker and follow, in general, the distribution of sediments at the surface, themselves causing thermal insulation of the rocks they rest on (Fig. 6.6). An additional temperature high is seen at the northern

edge of the model domain where the Nordmarka Plateau is found. Indeed, this local temperature high is only due to the depth below ground surface which is greater than for the surroundings. A marked temperature low is modelled in the southern and southeastern parts of the domain (corresponding to e.g. the Nesodden Peninsula and the Oppegård area) where the relatively low-radiogenic Precambrian basement crops out.

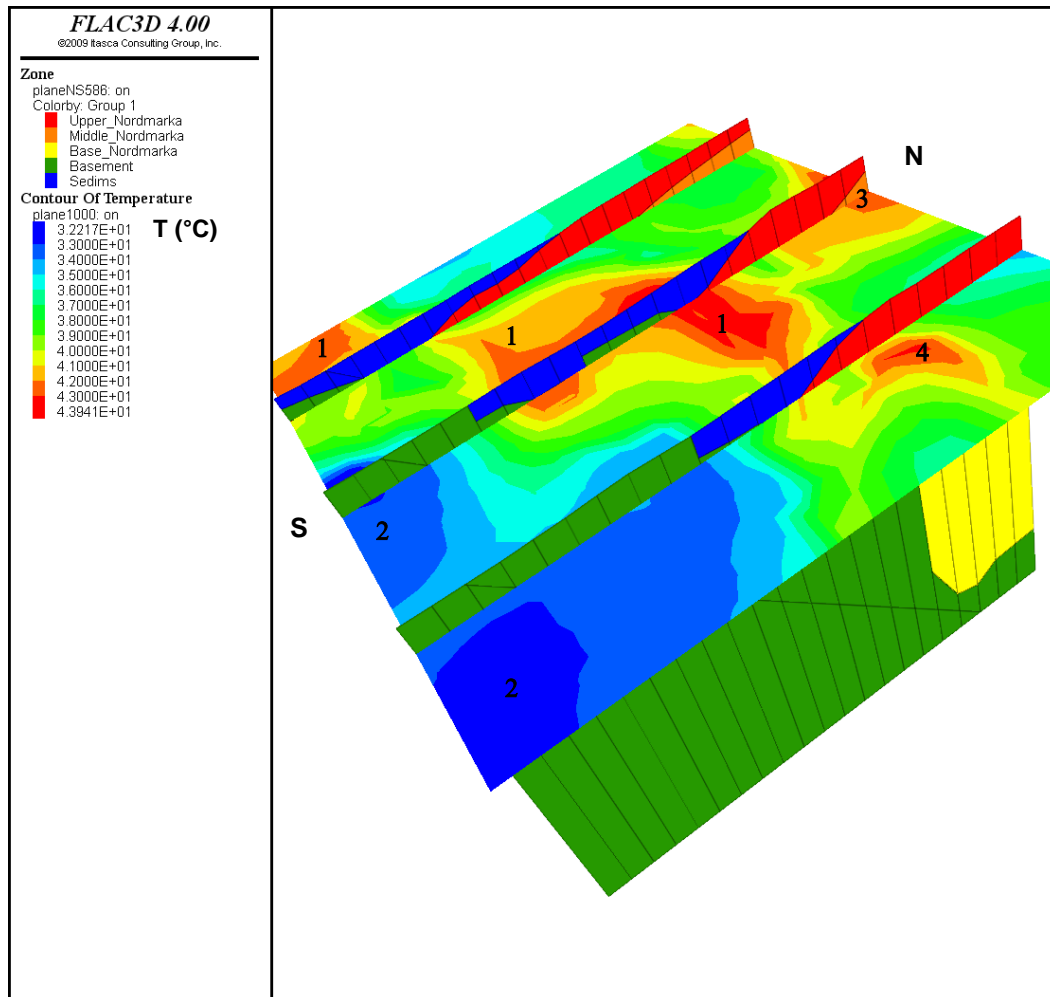


Figure 6.6. Modelled temperature distributions at 1 km depth below sea-level (“Optimistic” scenario, see Table 6.2) and vertical N-S cross sections depicting the structure of the crust. The temperature pattern is correlated to variations in structure and rock properties: (1) blanketing effect from relatively low conductive sediments, (2) low heat-generation Precambrian basement, (3) higher elevation of the rock surface (i.e. actual depth below ground level is 200-300 m more than for the surroundings) and (4) thick layer of granite with high heat generation.

At 5 km depth bsl, two temperature highs are modelled (Fig. 6.5). It is worth noting that these maxima differ by as much as 40°C from the “Pessimistic” scenario (i.e. maximum temperature 81°C) to the “Optimistic” one (i.e. maximum temperature 129°C). Figure 6.7 shows that the maxima are controlled by the thicknesses of the highly radiogenic Upper and Middle Nordmarka layers. Obviously, temperatures reach their maxima where the cumulative thickness of the two layers does so.

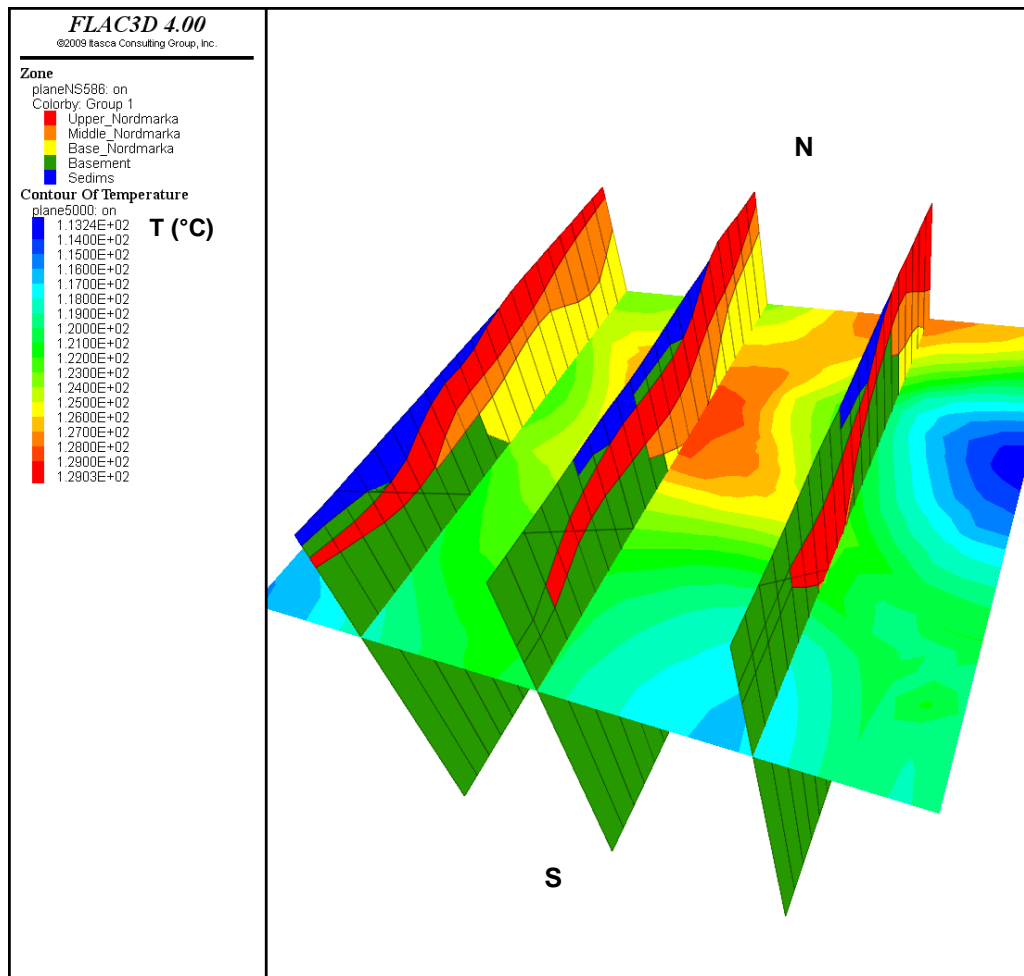


Figure 6.7. Modelled temperature distributions at 5 km depth below sea-level (“Optimistic” scenario, see Table 6.2) and vertical N-S cross-sections depicting the structure of the crust. Note that the highest temperatures occur below the most heat-productive rocks (i.e. Upper + Middle Nordmarka) where they reach maxima in cumulative vertical thickness.

As a final attempt, we modelled our “Preferred” scenario (Table 6.2 and Fig. 6.8). The temperature patterns at 1 and 5 km bsl remain basically unchanged compared to the previous scenarios, because the structure of the crust which has remained constant throughout the modelling study, dictates this pattern. The modelling suggests here average temperatures between 30°C and 34°C at 1 km depth bsl, in particular, below Oslo, Bærum and Asker. Local temperatures down to 28°C are predicted for basement areas and a maximum of 36°C is predicted close to the eastern edge of the modelled domain. At 5 km depth bsl, maximum temperatures up to 110°C are predicted below Oslo downtown.

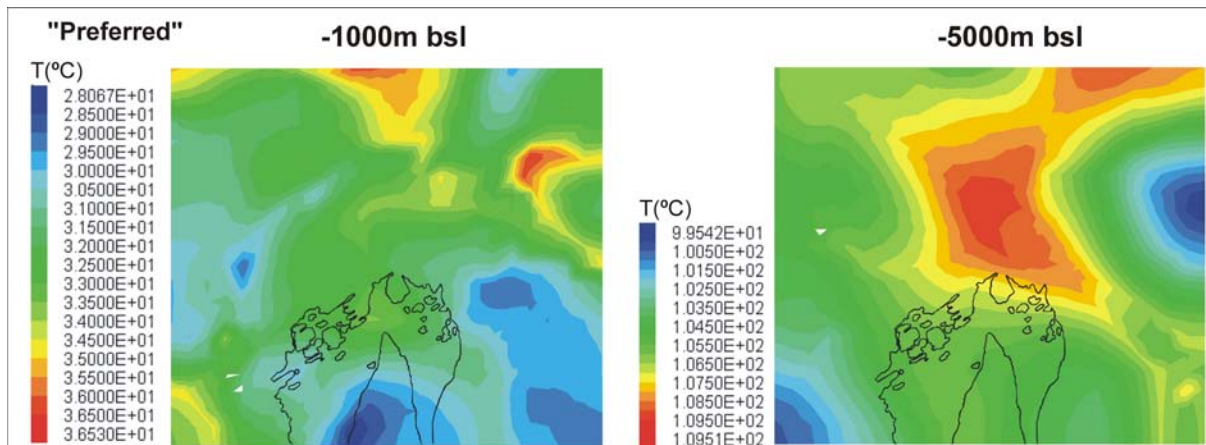


Figure 6.8. Modelled temperature distributions for the “Preferred” scenario (see Table 6.2) at 1 and 5 kilometres depth below sea-level. The apparent “positive” anomaly seen below the northern edge of the model at 1 km bsl is partly caused by the altitude of the Nordmarka Plateau (i.e. depth below ground surface is actually 1300-1400 m there).

6.4 Conclusions

The goal of the 3D thermal modelling study was to determine underground temperatures in the Oslo-Asker area. The modelling suggests that the highest temperatures at shallow depths (i.e. ~1 km depth) and at deeper levels (i.e. ~5 km depth) are found below the Cambro-Silurian sedimentary cover and below the locations where the upper layers of the Nordmarka Igneous Complex (i.e. Upper and Middle Nordmarka) are the thickest, respectively. Admittedly, the resolution of the 3D geophysical crustal model degrades with depth, rendering the location of the warmest areas more uncertain at 5 km depth with respect to 1 km depth.

In detail, the thermal modelling gives some hints on the temperatures that can be encountered at depth. Our “Pessimistic” and “Optimistic” modelling scenarios represent end-member cases, whose predictions should give the lowermost and uppermost underground temperatures, respectively. Our “Preferred” modelling scenario suggests temperatures between 30°C and 34°C at ~1 km depth below the Oslo-Asker area, in agreement with temperature gradients measured in the Arnestad borehole and to some extent with temperatures reported for the Rikshospitalet bh3 borehole. Temperatures in the range between 105°C to 110°C are predicted at ~5 km depth. Because it is a common feature in the three modelled cases, the most robust result is the relative lateral homogeneity in temperatures at 5 km depth, making site selection a less important factor when attempting to mine those depths. More significant lateral variations in temperature (i.e. 28% to 37%) are, however, predicted at 1 km depth for the whole modelled domain, indicating that selection of the drilling site is a more critical factor for exploiting the shallow geothermal resource.

A major conclusion of this study is that deep (i.e. ~5 km) temperatures, in the Oslo Region, remain relatively modest in all modelled cases and merely not of economic use with the present-day technology at hand. Temperatures at shallow depths appear high enough for direct

use and heating. It is, however, important to note that our conclusions are based on the present-day knowledge and that no reliable heat flow determination exists in the specific Oslo-Asker area.

7 CONCLUSIONS AND RECOMMENDATIONS

This study confirms that most rocks in the Bergen and Mongstad area show typical of the Norwegian basement (i.e. 1 to 3 $\mu\text{W}/\text{m}^3$) to low (i.e. less than 1 $\mu\text{W}/\text{m}^3$) heat generation values. The rocks in the vicinity of the Mongstad refinery are mainly amphibolitic gneisses and anorthosites with almost no heat generation at all. This suggests that medium to high enthalpy geothermal systems are much too deep below the ground surface to be of economic use there. The finding of very high concentrations of radioactive elements and, consequently, high heat generation rates for the Løvstakken Granite, five kilometres southwest of Bergen downtown, represents the most unexpected result of the study. A statistical analysis of the 45 measurements taken at sites distant of up to ~10 km shows average and median values of 10 and 9 $\mu\text{W}/\text{m}^3$ respectively, that are, to our knowledge, the highest ever measured in Norway. It is unknown how concentrations in radioactive elements decay with depth in the Løvstakken Granite, which is primordial while attempting to estimate heat flow values and temperatures in the deep underground. Two points are, however, interesting to note. Firstly, according to the geological interpretation, the granite extends at great depths and farther to the east below the Caledonian nappes. Secondly, conservative estimates using reasonable values lead to temperature gradients between 27 °C/km and 43 °C/km and temperatures between 135 °C and 215 °C at 5 km depth. The spread in values is obviously large but suggests anyway more favourable conditions for geothermal exploration as compared to most regions of Norway. This implies that economic underground temperatures may prevail below all of the municipality of Bergen.

Finally it is important to note that a similar radiometric study carried out in the framework of the “North Sea Crustal Onshore-Offshore Project” (Coop, financed by a consortium of companies including Statoil) in July 2010 has confirmed and extended our results. As a follow up of the present study and as part of the Coop project, we plan (1) to interpret the newly acquired potential field data and to build a 2D thermal model crossing the Løvstakken Granite and (2) to drill a 1-km deep hole in order to measure temperature gradients and refine our first-order estimates.

The goal of the 3D thermal modelling study was to determine underground temperatures in the Oslo-Asker area. The modelling suggests that the highest temperatures at shallow depths (i.e. ~1 km depth) and at deeper levels (i.e. ~5 km depth) are found below the Cambro-Silurian sedimentary cover and below the locations where the upper levels of the Nordmarka Igneous Complex (i.e. Upper and Middle Nordmarka) are the thickest, respectively. Admittedly, the resolution of the 3D geophysical crustal model degrades with depth, rendering the location of the warmest areas more uncertain at 5 km depth with respect to 1 km depth.

In detail, the thermal modelling gives some hints on the temperatures that can be encountered at depth. Our “Pessimistic” and “Optimistic” modelling scenarios represent end-member cases, whose predictions should give the lowermost and uppermost underground temperatures, respectively. Our “Preferred” modelling scenario suggests temperatures

between 30°C and 34°C at ~1 km depth below Oslo, Bærum and Asker, in agreement with temperature gradients measured in the Arnestad borehole and to some extent with temperatures reported for the Rikshospitalet bh3 borehole. Temperatures in the range between 105°C to 110°C are predicted at ~5 km depth. Because it is a common feature in the three modelled cases, the most robust result is the relative lateral homogeneity in temperatures at 5 km depth, making site selection a less important factor when attempting to mine those depths. More significant lateral variations in temperature (i.e. 28% to 37%) are, however, predicted at 1 km depth for the whole modelled domain, indicating that selection of the drilling site is a more critical factor for exploiting the shallow geothermal resource.

A major conclusion of this study is that deep (i.e. ~5 km) temperatures, in the Oslo Region, remain relatively modest in all modelled cases and merely not of economic use with the present-day technology at hand. Temperatures at shallow depths appear high enough to be used for e.g. heating purposes. It is, however, important to note that our conclusions are based on the present-day knowledge and that no reliable heat flow determination exists in the specific Oslo-Asker area.

8 REFERENCES

- Aalstad, I., Åm, K., Håbrekke, H. & Kihle, O. 1977: Aeromagnetic investigations along the Norwegian Geotraverse. In: K.S. Heier (ed.): *The Norwegian Geotraverse Project: A Norwegian contribution to the international upper mantle project and the international geodynamics project*. Geological Survey of Norway (NGU), 77-98.
- Anonymous 1989: Portable Gamma Ray Spectrometer: Model GR-256 with Model GPS-21 Detector manual. Exploranium G.S. Limited, Toronto, Canada, 61 pp.
- Clauser C. & Huenges, E. 1995: Thermal conductivity of rocks and minerals. In: Ahrens, T. J. (ed.) *Rock Physics and Phase Relations - a Handbook of Physical Constants*, AGU Reference Shelf, Vol. 3, pp. 105-126, American Geophysical Union, Washington.
- Ebbing, J., Afework, Y., Olesen, O. & Nordgulen, Ø. 2005: Is there evidence for magmatic underplating beneath the Oslo Rift? *Terra Nova* 17, 129–134.
- Ebbing, J., Skilbrei, J.R. & Olesen, O. 2007: Insights into the magmatic architecture of the Oslo Graben by petrophysically constrained analysis of the gravity and magnetic field. *Journal of Geophysical Research* 112, B04404, doi:10.1029/2006JB004694.
- Elvebakk, H. 2007: NGU Well logging 2006-2007. In Olesen et al. KONTIKI Final Report, CONTInental Crust and Heat Generation In 3D. NGU Report 2007.042, p. 43-62.
- Fugro Airborne Surveys Central Region 2003: Logistics report, fixed wing borne magnetic, radiometric and VLF-EM survey in the Oslo region, southern Norway. *Report FCR 2241*.
- Haenel, R., Grønlie, G. & Heier, K.S. 1979: Terrestrial heat-flow determination in Norway and an attempted interpretation. In V. Cermak and L. Rybach (eds.), *Terrestrial heat flow in Europe*, 232-240, Springer-Verlag, Berlin.
- Haenel, R., Rybach, L. & Stegena, L. 1988: *Handbook of Terrestrial Heat-Flow Determination*. Dordrecht, Kluwer Academic Publishers, 125-142.
- Heier, K.S. 1977: *The Norwegian Geotraverse Project: A Norwegian contribution to the international upper mantle project and the international geodynamics project*. Geological Survey of Norway (NGU), Trondheim.
- Heincke, B.H., Watson, R.J. & Møller, T. 2009: Determination of altitude-dependence of standard spectra and stripping ratios for the GR820 Airborne Gamma Ray Spectrometer. *NGU Report 2009.042*.
- Hurter, S. & Haenel, R. 2002: *Atlas of geothermal resources in Europe*. Office for Official Publications of the European Communities, Luxembourg.
- Kinck, J.J., Husebye, E.S. & Larsson, F.R. 1993: The Moho depth distribution in Fennoscandia and the regional tectonic evolution from Archean to Permian times. *Precambrian Research* 64, 23-51.
- Korhonen, J.,V., Aaro, S., All, T., Nevanlinna, H., Skilbrei, J.R., Säävuori, H., Vaher, R., Zhadanova, L. & Koistinen, T. 2002: *Magnetic anomaly map of the Fennoscandian shield 1: 2 000 000*. Geological Surveys of Finland, Norway and Sweden and Ministry of Natural Resources of Russian Federation.
- Korsman, K., Korja, T., Pajunen, M., Virransalo, P. & GGT/SVEKA Working Group 1999: The GGT/SVEKA Transect: Structure and evolution of the continental crust in the Paleoproterozoic Svecofennian Orogen in Finland. *International Geology Review* 41, 287-333.
- Lutro, O. & Nordgulen, Ø. 2004: Oslofeltet, berggrunnskart, 1.250.000, Geological Survey of Norway (NGU), Trondheim.
- Midttømme, K., Ramstad, R.K., Elvebakk, H., Koziel, J., Lutro, O., Nordgulen, Ø., Olesen, O., Slagstad, T. & Wissing, B. 2007: Thermal conductivity measurements. KONTIKI

- Final Report, CONTInental Crust and Heat Generation In 3D. *NGU Report 2007.042*, 77-108.
- Musæus, T.E., Midttømme, K., Hauge, A. & Müller, J. 2010: Deep geothermal demonstration project in Oslo. *ER3: Terrestrial heat flow: From Geodynamics to Society, 29th Nordic Geological Winter Meeting*, Oslo 11-13 Jan. 10.
- Olesen, O., Reitan, M. & Sæther, P.O. 1993: Petrofysisk database PETBASE 3.0, Brukerbeskrivelse. Norges geologiske undersøkelse Internal Report, 93.023, 74 pp.
- Olesen, O., Gellein J., Håbrekke H., Kihle O., Skilbrei J. R., & Smethurst M. 1997: *Magnetic anomaly map Norway and adjacent ocean areas, scale 1:3 million* Geological Survey of Norway (NGU), Trondheim.
- Olesen, O., Balling, N., Barrère, C., Breiner, N., Davidsen, B., Ebbing, J., Elvebakk, H., Gernigon, L., Koziel, J., Lutro, O., Midttømme, K., Nordgulen, Ø., Olsen, L., Osmundsen, P.T., Pascal, C., Ramstad, R.K., Rønning, J.S., Skilbrei, J.R., Slagstad, T. & Wissing, B. 2007: KONTIKI Final Report, CONTInental Crust and Heat Generation In 3D. *NGU Report 2007.042*.
- Pascal, C., Elvebakk, H. & Olesen, O. 2010: An assessment of deep geothermal resources in Norway. *Proceedings of the World Geothermal Congress, Bali, Indonesia, 25-30 April 10*.
- Ragnhildstveit, J. & Helliksen, D. 1997: Geologisk kart over Norge, berggrunnskart Bergen, 1.250.000, Geological Survey of Norway (NGU), Trondheim.
- Roy, R.F., Blackwell, D.D. & Birch, F. 1968: Heat generation of plutonic rocks and continental heat-flow provinces. *Earth and Planetary Sciences Letters* 5, 1-12.
- Rybach, L. 1988: Determination of heat production rate. In: Haenel, R., L. Rybach & L. Stegena eds. *Handbook of Terrestrial Heat-Flow Determination*. Dordrecht, Kluwer Academic Publishers, 125-142.
- Skilbrei, J.R., Kihle, O., Olesen, O., Gellein, J., Sindre, A., Solheim, D. & Nyland, B. 2000: Gravity anomaly map Norway and adjacent ocean areas, scale 1:3 Million. Geological Survey of Norway, Trondheim.
- Slagstad, T. 2008: Radiogenic heat production of Archaean to Permian geological provinces in Norway. *Norwegian Journal of Geology* 88, 149-166.
- Slagstad, T., Balling, N., Elvebakk, H., Midttømme, K., Olesen, O., Olsen, L. & Pascal, C. 2009: Heat flow measurements in Late Palaeoproterozoic to Permian geological provinces in south and central Norway and a new heat-flow map of Fennoscandia and the Norwegian-Greenland Sea. *Tectonophysics*, 473, 341-361.
- Smethurst, M., Strand, T., Finne, T.E. & Sundal, A.V. 2006: Gammasppektrometriske flymålinger og radon. *Strålevern Rapport 2006.12*.
- Tryti, J. & Sellevoll, M.A. 1977: Seismic crustal study of the Oslo Rift. *Pure and Applied Geophysics* 115, 1061-1085.

9 APPENDIX A: LITHOLOGIES PENETRATED IN THE RIKSHOSPITALET BH3 DRILLHOLE

TD (m)	bergart	beskrivelse
55	Sandstein	Grågrønt sediment, finkornet sandstein(?)
58	Skifer	Grønlig grå sediment, ksp i tynne stikk
60	Skifer	Grønnlig sediment
800	Svartskifer	Skiferfragment, ikke fullt så mørke som i prøvene fra 810 og 820, enkelte skiferfragment har det stenglige mineraletn noen fragment rustfarget
810	Alunskifer	Svarte skiferfragment og klare stenglig nåleforma mineral, zeolitt(?) og svovel- og kobberkiskorn
820	Alunskifer	Svarte skiferfragment og klare stenglig nåleforma mineral, zeolitt(?)
845	Alunskifer	Svarte skiferfragment og stenglig nåleforma mineral, zeolitt(?)
850	Alunskifer	Svarte skiferfragment og stenglig nåleforma mineral, zeolitt(?)
855	Alunskifer	De fleste fragmenta ser ut til å være bergartsfragment, skifer, farger fingrene svart
870	Skifer	De fleste fragmenta ser ut til å være av skifer, noen få kvartskorn
876	Skifer	Fleste fragmentene er av finkornig gråbrunlig bergart, små fragment av kvarts og plagioklas
882	paragneis	Kvarts, plagioklas og mye mørke mineral
890	paragneis	kvarts, plagioklas og finkorna mørke mineral
900	paragneis	Kvarts, plagioklas, biotitt, noe granat og skiferfragment
901	paragneis	Kvarts, plagioklas, noe biotitt og litt granat, og skiferfragment
910	paragneis	Kvarts, plagioklas og noe granat, det er en del mørke skiferbiter i prøven
930	paragneis	Kvarts, plagioklas, biotitt, granat
940	paragneis	Kvarts, plagioklas og noe biotitt og granat og noen skiferfragment
950	paragneis	Kvarts, biotitt, plagioklas, granat og skiferfragment
960	paragneis	Kvarts, biotitt, plagioklas granat, lite biotitt og granat, hovedsakelig kvarts og plagioklas
970	paragneis	Kvarts, biotitt, plagioklas granat, mest plagioklas(?), mindre biotitt enn i 1000
978	paragneis	Kvarts, plagioklas, biotitt, granat og skiferfragment
1000	paragneis	Kvarts, biotitt, plagioklas granat, mest plagioklas(?)
1030	paragneis	Kvarts, plagioklas, biotitt og finkornete grå kvartsittiske(?) fragment
1040	paragneis	Kvarts, plagioklas og noe biotitt (meget lys prøve)
1050	paragneis	Hovedsakelig kvarts og plagioklas og noen få amfibolkorn(?)
1060	granittisk gneis	Kvarts, K-feltpat og litt biotitt og amdre m.m. (amfibol?)
1090	granittisk gneis	Kvarts, K-feltpat, plagioklas, biotitt, og andre m.m.
1090	granittisk gneis	Kvarts, plagioklas, biotitt og litt granat
1100	granittisk gneis	Kvarts, plagioklas (noen epoidotiserte korn eller skapolitt?) litt biotitt, granat og amfibol(?)
1110	granittisk gneis	Kvarts, plagioklas hovedsakelig, noe biotitt og amfibol(?)
1120	granittisk gneis	Kvarts, plagioklas, biotitt, amfibol, litt muskovitt og noen granater (få m.m.)
1130	granittisk gneis	Kvarts, plagioklas, biotitt, noen få m.m., biotitt, granat
1160	granittisk gneis	Kvarts, K-feltpat, plagioklas, biotitt
1170	granittisk gneis	Kvarts, K-feltpat, plagioklas, biotitt, amfibol(?)
1180	granittisk gneis	kvarts, K-feltpat, m.m. (amfibol?), plagioklas, svovelkis
1200	granittisk gneis	K-feltpat, plagioklas
1210	granittisk gneis	Mørk prøve med mange aggregat av biotitt og med noen K-feltpatkorn, kvarts og plagioklas(?=

1220	granittisk gneis	Kvarts, K-feltspat, plagioklas, biotitt
1230	granittisk gneis	Kvarts, mye K-feltspat og noe m.m.
1270	granittisk gneis	Kvarts, mye K-feltspat og noe m.m.
1279	granittisk gneis	Kvarts, plagioklas, K-feltspatkorn, biotitt og andre mørke mineral
1281	granittisk gneis	Kvarts, plagioklas, K-feltspatkorn, biotitt og andre mørke mineral
1315	granittisk gneis	Kvarts, K-feltspat, plagioklas og amfibol(?)
1329	granittisk gneis	Kvarts, K-feltspat, plagioklas og amfibol(?)
1350	granittisk gneis	Kvarts, K-feltspat, plagioklas, m.m. (litt biotitt)
1360	granittisk gneis	Kvarts, K-feltspat, plagioklas, m.m. (litt biotitt)
1370	granittisk gneis	Kvarts, K-feltspat, plagioklas, m.m. (litt biotitt)
1380	granittisk gneis	kvarts, K-feltspat, plagioklas, biotitt og andre m.m.
1384	granittisk gneis	Kvarts, plagioklas, litt K-feltsapt, biotitt
1393	granittisk gneis	Kvarts, plagioklas, litt K-feltsapt, biotitt
1400	granittisk gneis	Litt kvarts, plagioklas of m.m.(amfibol?)
1460	granittisk gneis	Kvarts, K-feltspat, plagioklas noe m.m.
1476	granittisk gneis	Kvarts, K-feltspat, plagioklas noe m.m.
1490	granittisk gneis	Kvarts, K-feltspat, plagioklas noe m.m.
1500	granittisk gneis	kvarts, K-feltspat, m.m.
1530	granittisk gneis	Kvarts, plagioklas, noen får K-feltspatkorn og en god del mørke mineral (biotitt?)
1550	granittisk gneis	Kvarts, K-feltspat og mørke mineral (ikke biotitt)
1560	granittisk gneis	Kvarts, K-feltspat og mørke mineral
